Journal of Energy Storage 114 (2025) 115667

Contents lists available at ScienceDirect

Journal of Energy Storage

journal homepage: www.elsevier.com/locate/est

Research papers

Zero-emission chemical sites – combining power purchase agreements with thermal energy storage

Marco Prenzel [a,*], Freerk Klasing [a], Stefan Kirschbaum [b], Thomas Bauer [a]

[a] German Aerospace Center, Institute of Engineering Thermodynamics, Linder Höhe, 51147 Cologne, Germany
[b] Gesellschaft zur Förderung angewandter Informatik e. V., Volmerstraße 3, 12489 Berlin, Germany

A R T I C L E I N F O

Keywords:
Utility system
Steam supply
Molten salt
Energy system optimization
Electrification
Curtailment

A B S T R A C T

The chemical industry is adopting increasingly ambitious greenhouse gas emission targets. This work examines the decarbonization concept of a chemical site utility system based on renewable power purchase agreements and green hydrogen. To this end, a model of a zero-emission utility system including all typical components, demand profiles and energy prices was developed. The model was used to investigate the effect of flexibility options such as curtailment, power-to-heat and thermal energy storage by means of energy system optimization. Sensitivity studies were carried out with respect to the green hydrogen price, thermal energy storage investment costs and on-site steam turbine capacity to gain a deeper understanding of the various influencing factors. Thermal energy storage, e.g. molten salt technology, can achieve cost savings up to 27 % through efficient integration of renewable electricity from PV and wind. Furthermore, the concept with thermal energy storage proved to be more resilient to variations in the green hydrogen price. In the best-case scenario, a 30 % higher green hydrogen price only results in a 6 % increase in annual expenditures. Even when very high investment costs are assumed, thermal energy storage still remains an integral component of the cost-optimal zero-emission utility system.

1. Introduction

The world is on course to miss almost all transformation targets in areas such as power generation, industry, transport and buildings that are needed to meet the 1.5 °C target of the Paris Climate Agreement [1,2]. With growing urgency to mitigate climate change, companies are starting to take this challenge into their own hands. With regard to the chemical industry, many big players have committed to ambitious greenhouse gas (GHG) emission targets or have even pledged to become climate-neutral within the next decade [3,4]. According to the GHG Protocol, emissions can be divided into three categories: Scope 1) Direct emissions from owned sources, for instance CO_2 from fuel combustion or industrial production; Scope 2) Indirect emissions from energy purchases; Scope 3) Indirect emissions upstream and downstream of the company value chain (e.g. business travel, use of sold products and also GHG footprints from purchased raw materials) [5,6]. A major source of Scope 1 and 2 emissions in the form of CO_2 at chemical sites is the central utility system. Large cogeneration plants and steam boilers produce electricity and heat (steam) to power the chemical processes on site [7].

To reduce or even eliminate CO_2 emissions entirely, an important step could be a switch to low-CO_2 or green electricity. Partial electrification of energy-intensive industries such as chemicals, but also basic materials, textiles and steel is technologically feasible [8–12]. A switch to electricity has an impact on energy demand, CO_2 emissions and costs. For instance, the deployment of electric boilers could reduce energy intensity and CO_2 emissions from fossil based steam generation [13]. The increasing electricity demand, in turn, requires an expansion of transmission and distribution grids as well as investments into the grid connection and electrification of a chemical site [14]. Lastly, many industrial processes require continuous operation and therefore a high security of energy supply. Since low-cost green electricity is not always available, a reliable solution for a zero-emission industry must include other energy sources and technical solutions in addition to electrification [15].

Another option could be carbon capture and storage (CCS). Of the available solutions, post-combustion processes for cogeneration plants appear to be the most suitable due to their advanced development level and the possibility of retrofitting existing plants [16,17]. Investments in CCS technologies affect production costs. For example, the price of heat

* Corresponding author.
E-mail address: marco.prenzel@dlr.de (M. Prenzel).

https://doi.org/10.1016/j.est.2025.115667
Received 5 July 2024; Received in revised form 20 December 2024; Accepted 1 February 2025
Available online 15 February 2025

could more than double with the implementation of CCS (cost of transportation and storage of CO_2 included) [18]. Effective and sustainable storage of CO_2 is another challenge [19]. The storage load could be alleviated by utilization of the captured CO_2 as feedstock [20]. However, this approach is limited by the demand for CO_2 as feedstock by the considered chemical site. For these reasons, CCS was not considered further in this study.

A switch to CO_2-neutral fuels, such as green hydrogen is also feasible. This would entail investments in H_2-ready gas turbines and steam boilers. H_2-ready gas turbines are expected to be available on the market in the near future, and the original equipment manufacturers are gathering initial operating experience [21,22]. Hydrogen steam boilers are commercially available, at least on the small MW-scale [23,24]. The main obstacles to green hydrogen are availability, political framework conditions and cost uncertainties.

Finding optimal solutions for the decarbonization of utility systems is complex, as there are numerous strategies and technologies to choose from, as described above. Recent publications consider electrically charged thermal energy storage (TES) systems as flexibility options [25–30]. TES can enhance electrification of the heat supply and thus reduce operating costs. Inexpensive low-CO_2 or green electricity from the grid is stored in form of thermal energy and later used to generate steam in times of high electricity prices. In addition, this steam can also be used to regenerate electricity via steam turbines. Studies show that TES can be a key component in industrial utility systems (e.g. chemical site, iron foundry or steel mill) to reduce the operating costs under different market scenarios [25–29]. In addition, TES could also improve the potential of the utility system to provide control reserve for the grid [31,32]. Viable TES technologies include phase change materials (PCM), regenerators, thermochemical energy storage and molten salt [33]. High temperature TES is preferred for chemical sites because high-pressure steam can be generated, leading to maximum flexibility.

The use of TES to generate revenue through arbitrage or ancillary services and to reduce operating costs represents a reasonable flexibility option. However, it is not suitable for companies that are aiming for a zero-emission utility system in 2030–2035, for instance. The electricity mix will still be afflicted with CO_2 emissions at this time.

For this reason, a novel approach is investigated in this paper. Zero-emissions are achieved by the procurement of green electricity from power purchase agreements (PPA) and use of green hydrogen. The existing cogeneration plant of the utility system must be modified for operation with green hydrogen. This switch is required because security of energy supply to the chemical processes must be guaranteed even during longer periods without PV or wind electricity. The use of carbon offsets is not considered in this study. Energy storage should play a key role in integrating a higher share of electricity from PPAs, mitigating the use of more expensive green H_2. In principle, battery storage could also be used for this purpose. However, in this work, thermal energy storage is considered as a flexibility option, in particular due to its higher storage density compared to batteries. The storage density of e.g. molten salt thermal energy storage can reach around 1300 kWh_{th}/m^2 (Assumptions used for estimation: Two tanks with 40 m diameter, 13 m height and 300–560 °C temperature range [34], specific heat capacity of 1550 J/kgK and density of 1800 kg/m^3 [35]). The Victorian Big Battery in Geelong, Australia, can be used as a reference for large batteries [36]. The storage density of this battery system amounts to roughly 25 kWh_{el}/m^2 (estimated from aerial photographs). Even though electricity and thermal energy storage are not directly comparable, the difference in storage density is nevertheless significant. This can be critical for application at chemical sites, where construction space is very limited. Battery systems have a higher efficiency for power-to-power operation compared to TES, but this advantage is mitigated by high investment costs [37] and the fact that the majority of the energy demand at the chemical site is heat. For power-to-heat operation with storage, both TES and batteries display similar levels of efficiency. Albeit the arguments above do not conclusively rule out the battery option, this work focuses on the more applicable concept with TES.

A model of a zero-emission chemical site was developed to investigate the proposed concept. The optimal dimensioning of PPAs, TES and electric steam boilers as well as the optimal operation of the utility system are determined with the commercial energy system optimization software TOP-Energy®. Previous scientific work on optimizing the steam and electricity supply at chemical sites with PPAs and TES could not be identified. The solutions are evaluated in terms of energy mix (share of green hydrogen and electricity), annual operating costs (annuity) and optimal sizing of components.

2. Methods

This section is structured into the model definition of the zero-emission utility system (2.1), investment cost estimations for all components (2.2), cost assumptions for PPAs (2.3) and green hydrogen (2.4), method and assumptions for energy system optimization (2.5) as well as an overview of all optimizations carried out within this work (2.6).

2.1. Zero-emission utility system model

A model of a zero-emission utility system was developed for this work. The structure can be seen in Fig. 1. The utility system must cover the energy demand of the chemical processes on site at all times.

These chemical processes are not modeled in detail, instead they are represented by demand profiles of a typical chemical site in Germany. An electricity, medium-pressure (MP, 31 bar and 370 °C) and low-pressure (LP, 6 bar and 210 °C) steam demand can be distinguished. The average demands shown in Fig. 1 were taken from [39] and then used to develop representative annual time series for the electricity and steam demand with an hourly resolution (as described in [38]). Water (15 °C) is injected into the LP and MP steam to lower the temperature before it is delivered to the end-use processes. The utility system also includes a high-pressure (HP, 530 °C, 110 bar) steam line to increase the on-site power generation capacity. A hydrogen gas turbine (GT) with heat recovery steam generators (HRSG), two large hydrogen gas boilers (GB) and steam turbines (ST) serve as electricity and steam producers, when green electricity is not available. The hydrogen-fired components were designed with EBSILON Version 15.02 [40]. The minimum local temperature difference in any heat exchanger (economizer, evaporator and superheater) between the flue gas and water side was kept above 10 K. Internal preheating was considered in the design to maximize efficiency (for the definition of all component efficiencies refer to [38]). The resulting efficiencies can be seen in Fig. 1. Note that the GB efficiency surpasses 100 %. This is due to the fact that the efficiency is defined based on the lower heating value (LHV) and parts of the condensation heat can be recovered in the economizer of the GB. The steam produced by the HRSGs and GBs can drive the available high-pressure (HP-ST), medium-pressure (MP-ST) and low-pressure (LP-ST) steam turbines. On-site power generation is sufficient to cover the electricity demand even at peak times. This enables the utility system to provide sufficient steam and electricity even when there is no electricity available from PV and wind. The operation of the GT and GBs is affected by the temperature of ambient air used for combustion. For this study, North Rhine-Westphalia, Germany was selected as the hypothetical location for the utility system. A forecast data set from the German Meteorological Service (Deutscher Wetterdienst) was included in the model (Test Reference Year 2031–2060, Leverkusen Germany) [41].

Ideally, a large share of the energy demand is met via PV or wind PPAs. Electricity from PPAs may be curtailed as part of operational optimization. Renewable electricity is used first and foremost to cover the electricity demand of end-use processes. During this time, the steam turbines are switched off and steam is distributed from the high to the lower pressure lines with pressure reducing stations. The steam supply can be electrified if surplus electricity is available. Two options were considered: 1) Direct electrical steam generation with a power-to-heat

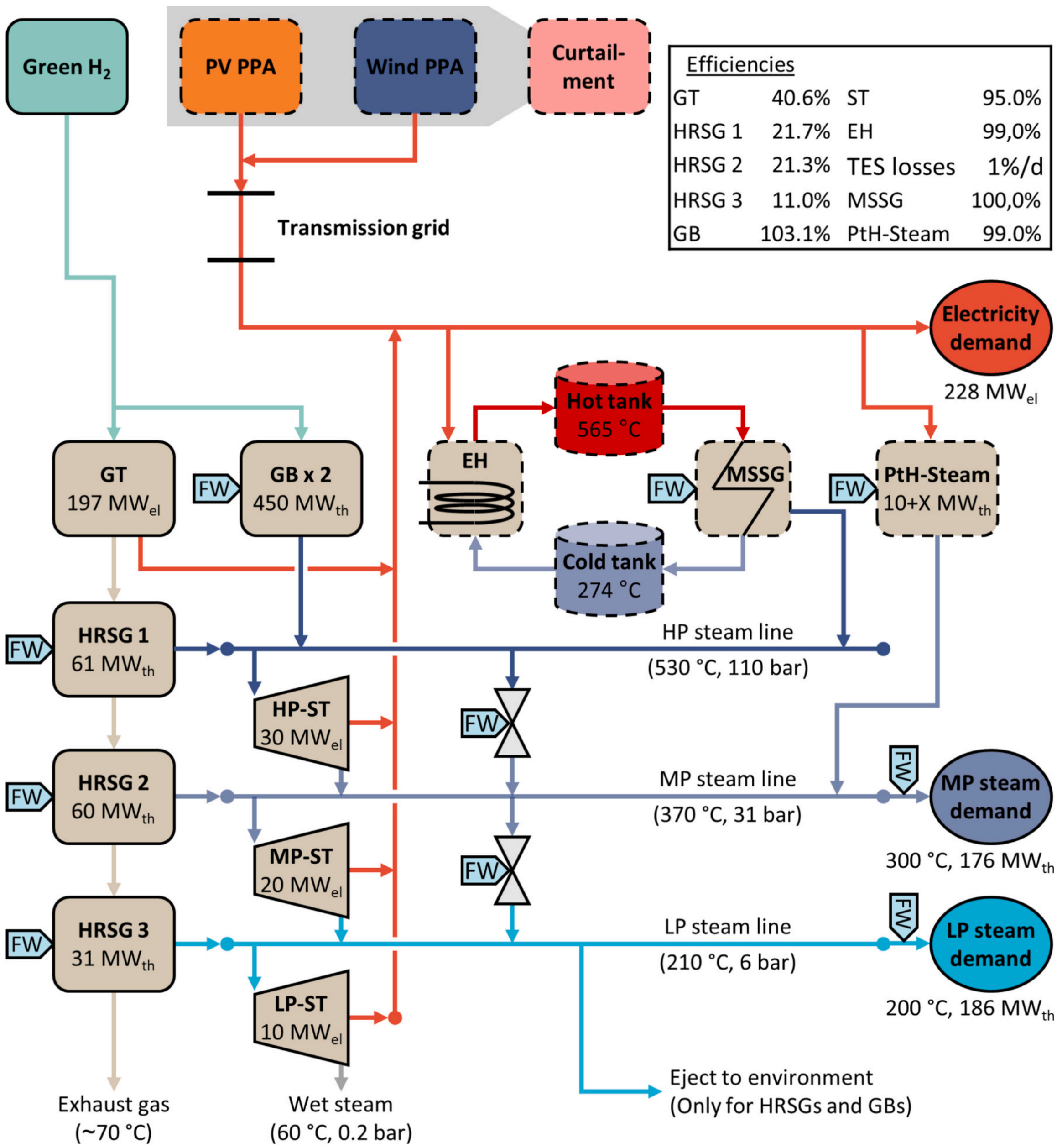

Fig. 1. Zero-emission utility system model including molten salt TES, in part adapted from [27,38]. Abbreviations: EH: Electric heater, FW: Feedwater, GB: Gas boiler, GT: Gas turbine, HP: High-pressure, HRSG: Heat recovery steam generator, LP: Low-pressure, MP: Medium-pressure, MSSG: Molten salt steam generator, PtH-Steam: Power-to-heat for steam, ST: Steam turbine.

steam generator (PtH-Steam); 2) Utilization of a TES system with a steam generation that can be decoupled from the power supply. Two-tank molten salt TES is a viable technology for chemical site utility systems due to its high level of maturity, scalability and suitable storage temperature [34]. During charge, molten salt from the cold tank is heated in an electric heater (EH) and then stored in the hot tank. During discharge, hot molten salt is used to generate high-pressure steam in a molten salt steam generator (MSSG). The TES system has two operation modes: 1) PtH mode: Electric heater and steam generator are operated concurrently with the same power to directly produce steam from renewable electricity without storage; 2) Charge and discharge mode: At times of high renewable generation, the storage system is charged. At a later point in time, when less PV and wind power is available, the storage system is discharged [27]. With a large electric heater, direct steam generation and storage of thermal energy can occur simultaneously.

The utility system has the option to release low-pressure steam to the environment. This measure is applied in cases with low renewable electricity production, high electricity demand and low steam demand. The steam turbines must be ramped up to maximum electricity production and the amount of steam in the utility system exceeds the total steam demand. As a consequence, the excess steam is blown off. This option is only available for steam produced by the HRSGs or GBs. Otherwise, PPA electricity could be curtailed by transmission to the utility system, conversion into steam and immediate release to the environment. This strategy is not tenable because it would require an unnecessary and costly expansion of the transmission grids and grid connections.

Finally, the utility system model consists of existing, fixed components (solid line) and optional components with variable size (dashed line, named variable components in this work). The latter includes the PPAs, PtH-Steam and the three individual elements of the molten salt

Table 1
Investment cost estimates ("Total As-Spent Capital") used for the energy system optimization and green hydrogen price estimation.

Component	Symbol	Specific cost	References	Other included cost factors
PtH (PtH-Steam)	c_{PtH}	300 €/kW$_{th}$	[44–46]	Transformer, switchgear, cables
TES charge (Electric heater)	c_{EH}	300 €/kW$_{th}$	[45–48]	Transformer, switchgear, cables
TES storage (Hot and cold tank)	c_{TES}	35 €/kWh$_{th}$	[49]	Foundation, thermal insulation, pumps, balance of plant, ancillary components
TES discharge (Molten salt steam generator)	c_{MSSG}	150 €/kW$_{th}$	[47,49]	Piping, thermal insulation, steel structure, instrumentation
Alkaline electrolyzer (AEL)	c_{AEL}	700 €/kW$_{el}$	[50]	Power electronics, transformer, instrumentation, water purification, piping etc. (projected cost in 2030)

Table 2
Summary of PV and wind PPA cost data.

Variable	Specific cost	Comment
PV PPA electricity price	62.57 €/MWh	Incl. energy rate of 4.62 €/MWh
Wind PPA electricity price	66.66 €/MWh	Incl. energy rate of 4.62 €/MWh
Demand rate	57.87 €/kW$_{year}$	Based on maximum power transmitted to utility system within one year
Curtailment costs	138.71 €/MWh	Valid for both PV and wind electricity

TES system (charging, storage and discharging unit). These components can be freely dimensioned by the energy system optimization tool. In this model, a small 10 MW$_{th}$ PtH-Steam unit is already in operation and part of the existing utility system. Additional PtH-Steam capacity can be built on top.

Transmission lines from power plants to the utility system as well as H_2 pipelines are not considered as investment costs in this study. This assumption was made because it is unclear who will bear the necessary investments. Industry, grid operators and the government all have a stake in grid expansion and will each have to make a financial contribution in some form. The transmission lines within the utility system (e. g. for PtH-Steam and TES discharging unit) were included in the respective investment costs of the components.

2.2. Investment cost estimations

The investment costs of the PtH-Steam unit and the three molten salt TES subsystems are required inputs for the energy system optimization tool. In addition, a cost indication for electrolyzers is needed to derive a green hydrogen price later in this work. For this purpose, cost data from recent publications were compiled and used to estimate the total investment costs of the different components. In most cases, cost figures in the scientific literature more or less refer to so-called "Bare Erected Costs" (BEC). BEC include process equipment, supporting facilities and labor. To obtain more comprehensive cost estimates, literature data were extended with methods from [42] to determine the "Total As-Spent Capital" (TASC). It is expected that the prices for electrolyzers will decrease significantly in the period 2030–2035 compared to today's values. For this reason, projected costs for 2030 are considered in this paper. Alkaline electrolyzers (AEL) were selected here because they are expected to be less expensive compared to proton exchange membrane (PEM) electrolysis and solid oxide electrolyzer cells (SOEC) [43]. The learning curves for TES and PtH are not expected to be as pronounced. Therefore, current investment costs without learning curves are applied. The investment cost estimates, especially for TES and PtH steam, can therefore be regarded as conservative. The final investment cost indications used in this work are summarized in Table 1. The cost figures in Table 1 apply to large-scale installations. The effects of economies of scale are negligible for all technologies in this case.

2.3. Power purchase agreements

Power purchase agreements (PPAs) are long-term electricity purchase contracts concluded between an electricity producer (seller) and an electricity consumer (buyer). The quantity of electricity supplied, the electricity pricing structure and the contract duration are the main aspects of a PPA contract. However, the legal structure and electricity delivery scheme of PPAs may differ considerably [51]. This paper selects so-called Pay-as-Produced PPAs. Electricity is supplied to the consumer as generated by a renewable energy plant (PV or wind) at a fixed price per MWh. This form of PPA represents a true green electricity supply, since there is a clear temporal correlation between renewable electricity generation and consumption. Baseload PPAs, on the other hand, offer a fixed supply of electricity regardless of the current PV and wind output. Deviations between generation and the contractually agreed delivery volumes are balanced through the spot market. While researching this topic, it became apparent that baseload PPAs will probably be offered less frequently in the future. Sellers of PPAs are not willing to take the risk of having to compensate for an electricity underproduction on an increasingly volatile spot market. It is expected that sellers would pass on the risk via increased baseload PPA costs. This will probably result in poor predictability and higher costs for baseload PPAs. The abbreviation PPA will hereinafter be used as **"pay-as-produced PPA"** for simplification. Baseload PPAs are not considered in the remaining work due to the above arguments.

The electricity costs from Pay-as-Produced PPAs were obtained from the "enervis PPA-Preistracker" (PPA price tracker) [52]. The price tracker is a tool typically used by companies to check reasonable PPA prices before entering into contract negotiations with sellers. The PPA prices in this tool depend on the start year, the duration of the contract and the date on which the PPA contract is closed. The date of contract conclusion is relevant because cost indications on the futures market, which are constantly changing, influence the PPA price. Average electricity prices for PV and onshore wind PPAs were derived on the basis of contracts with different start times, durations and date of contract conclusion (see PPA electricity prices in Table 2). Electricity consumers must pay grid fees when electricity is transferred to them via the transmission grid. First, an energy rate per MWh supplied has to be paid in addition to the PPA price. Second, a demand rate is due, which depends on the maximum power that is transmitted to the utility system at any given point in time within a year. Average energy and demand rates were determined using historical data (2019–2023) from the North Rhine-Westphalian transmission grid operator Amprion (see grid fee values in Table 2) [53,54].

In addition to the electricity prices, annual electricity generation profiles with hourly resolution were developed for PV and wind power plants. To this end, a list of 15 large ground-mounted PV systems and 15 large wind turbines, spread across the entire state of North Rhine-

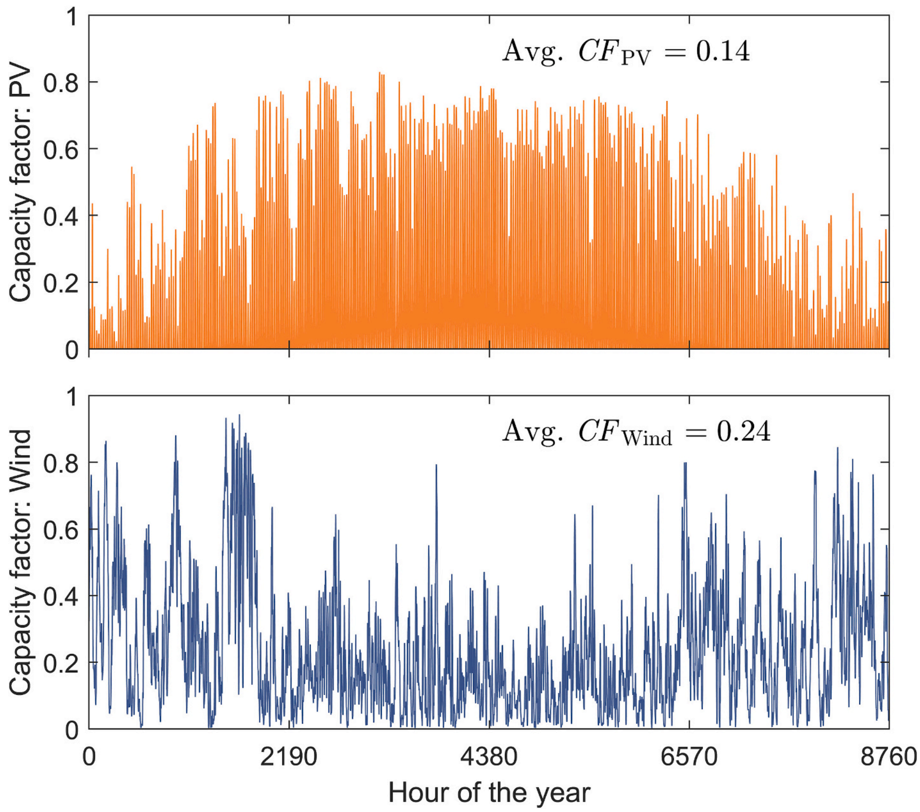

Fig. 2. PV and wind electricity generation profiles.

Westphalia, was compiled [55]. The generation profiles of these installations were then determined with methods from [56–58]. Average profiles were developed because a single PV system or a wind farm would not be able to supply sufficient electricity for the utility system. Averaged profiles are therefore more realistic. The resulting generation profiles can be seen in Fig. 2.

Multiplying the capacity factor with the installed capacity of a PV or wind installation yields the electricity production:

$$\overrightarrow{P}_{\mathrm{el}} = \overrightarrow{CF} \bullet P_{\mathrm{inst}}. \tag{1}$$

Here, $\overrightarrow{CF}$ is a vector containing the capacity factors for an entire year with an hourly resolution.

The average capacity factor of wind power plants with a value of 0.24 is higher than that of PV systems with 0.14. Assuming installations with identical installed peak capacity (e.g. in $\mathrm{MW_{peak}}$), wind produces more electricity than PV over the course of the year. It can be advantageous to curtail PV and wind power. This measure could stabilize the grid, reduce demand rate cost and enable the integration of larger volumes of renewable electricity. Curtailment costs were derived from information provided by the Bundesnetzagentur (German Federal Network Agency) [59].

All cost data with regard to PV and wind PPAs are summarized in Table 2. For economic reasons, wind power should be curtailed first because the electricity price of wind PPAs is higher. The curtailment costs are the total costs to be paid and not an additional charge on top the PPA electricity price.

2.4. Green hydrogen

The European Parliament's Renewable Energy Directive sets out criteria for the production of green hydrogen. Electricity for the production of green hydrogen is only recognized as renewable if the criteria of additionality as well as geographical and temporal correlation are satisfied. Additionality is given if the electricity is procured through renewable PPAs from installations that have been put into operation not longer than 36 months before the water electrolysis. The geographical correlation is fulfilled if the electrolyzer and the PV and/or wind power plants associated with the PPAs are located in the same bidding zone. From 2030 onwards, the renewable electricity must be consumed by the electrolyzer within one hour of being generated in order to comply with the temporal correlation criterion. Exceptions are possible, but the criteria described above apply in most cases [60]. The Pay-as-Produced PPAs described in the previous subsection meet all criteria to produce green hydrogen, provided that the electrolyzer is located in the Germany/Luxembourg bidding zone. Hence, a green hydrogen price can be derived, which is directly correlated to the cost of renewable electricity. The levelized cost of green hydrogen (LCOH) can be calculated as follows:

$$c_{\mathrm{H2}} = \frac{P_{\mathrm{AEL}} c_{\mathrm{AEL}} + \sum_{y=1}^{y=n} \frac{C_{\mathrm{El}} + C_{\mathrm{Curt}} + C_{\mathrm{Grid}} + C_{\mathrm{St\&Dist}} + C_{\mathrm{O\&M}}}{(1+i)^{y}}}{\sum_{y=1}^{y=n} \frac{m_{\mathrm{H2}}}{(1+i)^{y}}}. \tag{2}$$

The expenditure side (numerator) includes the investment cost for the electrolyzer (product of installed capacity P_{AEL} and specific cost c_{AEL}) as well as the annual expenses for PPA electricity C_{El}, curtailment C_{Curt}, grid demand rate C_{Grid}, storage & distribution of hydrogen $C_{\mathrm{St+Dist}}$ and operation & maintenance $C_{\mathrm{O\&M}}$. On the revenue side, there is the

Table 3
Assumptions for LCOH calculation.

Variable	Estimated values	References
AEL efficiency	68 % (lower heating value)	[43]
AEL lifetime	12 years	[43,61,62]
Spec. storage & distribution cost	1.5 €/$\mathrm{kg_{H2}}$	[63]
Spec. operation & maintenance cost	2 %Invest/year	[43,64]
Interest rate	8 %	[65,66]

amount of green hydrogen produced annually m_{H2}.

Expenses and revenue are discounted with the interest rate i and then added up over the lifetime of the AEL n. Further assumptions must be made in order to calculate the annual cost contributions and hydrogen production. These are summarized in Table 3.

To calculate the LCOH, a ratio between the installed PV and total capacity (wind and PV) is introduced, which is here referred to as the PV share R_{PV}:

$$R_{PV} = \frac{P_{PV,inst}}{P_{PV,inst} + P_{Wind,inst}} \text{ with } 0 \leq R_{PV} \leq 1. \quad (3)$$

A value of $R_{PV} = 0$ means that only wind PPAs are used to generate green hydrogen. $R_{PV} = 1$ indicates that green hydrogen is produced exclusively through PV PPAs. To clarify, the ratio R_{PV} is calculated with the installed capacities of PV and wind power plants and not with the volumes of PV or wind electricity used for H_2 production. The LCOH is not affected by the absolute values of $P_{PV,inst}$ and $P_{Wind,inst}$, as size-independent specific cost are assumed for the AEL. This allows the green hydrogen price to be calculated depending on the PV share R_{PV}. The method is described in the following:

- The PV share R_{PV} is varied between 0 and 1 in predefined increments.
- For a given value of R_{PV}, the installed PV and wind power plant capacities $P_{PV,inst}$ and $P_{Wind,inst}$ are calculated according to Eq. (3). To this end, the combined output of the PV and wind power plants associated with the PPAs was simply scaled to a total of 1 MW_{peak} ($P_{PV,inst} + P_{Wind,inst} = 1$ MW).
- The PV and wind generation profiles are determined using the capacity factors of Fig. 2 and Eq. (1).
- Equations are set up for the annual cost components C_{El}, C_{Curt}, C_{Grid}, $C_{St\&Dist}$ and $C_{O\&M}$ as well as the annual hydrogen production m_{H2} as a function of the installed electrolyzer capacity P_{AEL}. As a result, the LCOH, according to Eq. (2), becomes a function of P_{AEL}.
- The LCOH is minimized for a given value of R_{PV} with the installed electrolyzer capacity P_{AEL} as the optimization variable.

The mathematical problem was set up in MATLAB R2020b [67] and minimized using the nonlinear programming solver “fminsearch” [68].

The resulting minimal LCOH over the PV share R_{PV} can be seen in Fig. 3. The minimum LCOH of 6.85 €/kg (205.58 €/MWh_{LHV}) can be achieved with a PV share R_{PV} of 0.44. Due to the higher capacity ratio of wind, wind energy contributes 68 % to green hydrogen production in the minimum LCOH case. The optimal electrolyzer capacity P_{AEL} is 0.37 MW in that instance. As a result of this preliminary study, a constant hydrogen price of 6.85 €/kg was used for the optimization of the zero-emission utility system.

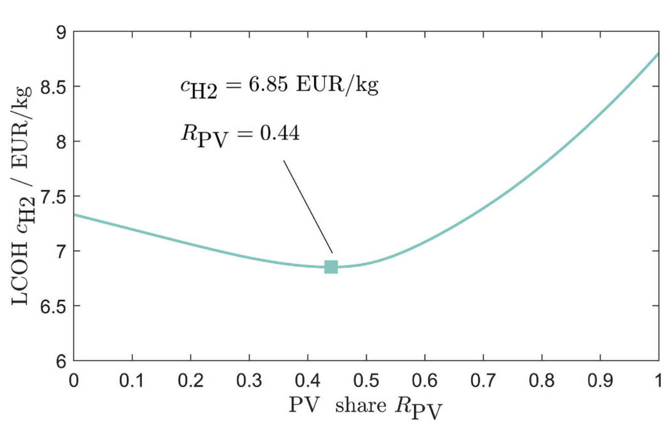

Fig. 3. Minimized levelized cost of hydrogen (LCOH) depending on the PV share R_{PV}.

2.5. Method and assumptions for energy system optimization

The zero-emission utility system, as shown in Fig. 1, was modeled in the software TOP-Energy® version 3.1.0 [69] for structural and operational optimization. Fig. 4 provides an overview of the input parameters (left), the energy system design optimization (middle) and the optimization results (right).

Most of the input parameters were discussed in previous subsections. Operation and maintenance costs for the TES units and PtH-Steam are set to 0.3 %Invest/year. Due to the higher technology readiness level, a lower value was applied here compared to the AEL (see Table 3). The operation and maintenance cost include an additional € 150,000/a for the personnel required to operate each new component (PtH steam and TES) [27]. The number of periods is set to $n = 10$ years. This is a typical time frame in which companies evaluate the impact of an investment. This implies that energy system optimizations were carried out for a representative year and the results were then assumed constant for the following 10 years to determine the target function. The target function of the optimization in TOP-Energy® is the annuity a:

$$a = AF \bullet CAPEX + OPEX, \quad (4)$$

with the annuity factor

$$AF = \frac{(1+i)^n \bullet i}{(1+i)^n - 1}. \quad (5)$$

The capital expenditures are the sum of all investments for PtH-Steam, electric heaters, thermal energy storage and molten salt steam generator. The individual investment costs are calculated by multiplying the installed power ($\dot{Q}$) or storage capacity (ΔU) with the specific cost c:

$$CAPEX = \dot{Q}_{PtH} c_{PtH} + \dot{Q}_{EH} c_{EH} + \Delta U_{TES} c_{TES} + \dot{Q}_{MSSG} c_{MSSG}. \quad (6)$$

The operational expenditures are the sum of all annual variable and fixed operating costs including PV electricity, wind electricity, green hydrogen, curtailment, demand rate as well as operation & maintenance (including personnel):

$$OPEX = C_{PV,el} + C_{Wind,el} + C_{H2} + C_{Curt} + C_{Grid} + C_{O\&M}. \quad (7)$$

In the end, the CAPEX and OPEX depend on the installed capacities of the PV and wind power plants associated with the PPAs, the size of the optional components (PtH-Steam and all subsystems of the molten salt TES) and the operating strategy of the utility system. In consequence the objective of TOP-Energy® is to minimize the annuity as a function of the above-mentioned influencing factors. The optimization problem represents a mixed integer linear program (MILP). TOP-Energy® solves the mathematical problem by means of the Gurobi optimizer [70]. The optimization results are evaluated, inter alia, in terms of energy mix, composition of the annuity and component sizing. Furthermore, a share of curtailment R_{Curt} is introduced to evaluate how much renewable electricity is curtailed in different scenarios:

$$R_{Curt} = \frac{sum\left\{\vec{P}_{Curt,el}\right\}}{sum\left\{\vec{P}_{PV,el} + \vec{P}_{Wind,el}\right\}}. \quad (8)$$

The numerator represents the sum of renewable electricity that is curtailed for operational optimization. The denominator is the maximum renewable electricity produced by PV and wind power plants without curtailment. A share of curtailment of $R_{Curt} = 0$ indicates that no renewable electricity is curtailed and sites for PV and wind power plants are used to their full potential. This indicator cannot be used to make a conclusive assessment of the renewable's utilization, as green hydrogen production is also subject to losses due to electrolyzer efficiency and curtailment. Nevertheless, R_{Curt} is a useful value to draw conclusions

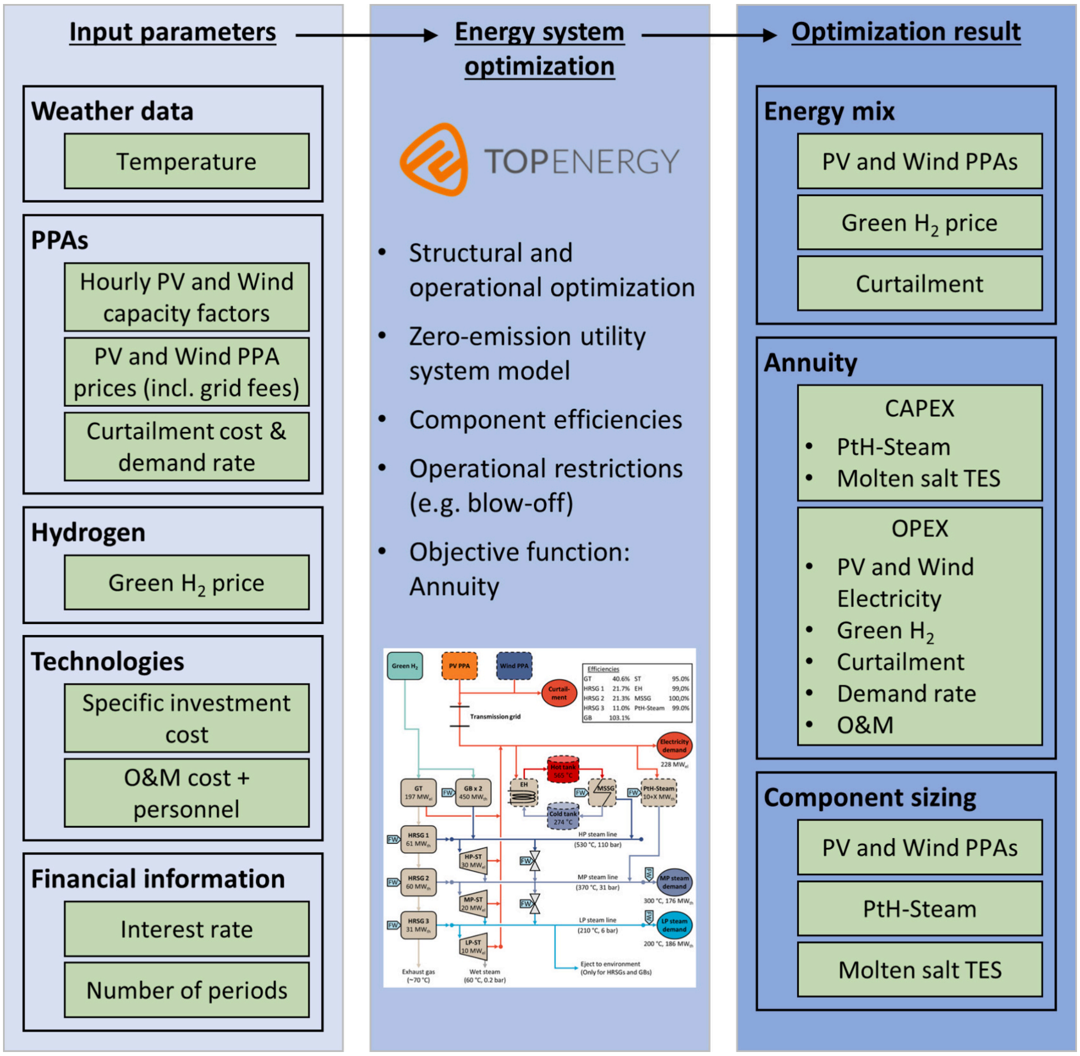

Fig. 4. Optimization methodology for the zero-emission utility system including the required input parameters and optimization results.

about how efficiently PV and wind electricity can be integrated into the utility system with PtH and TES.

2.6. Conducted optimizations

Table 4 contains details of all the optimizations carried out. A total of four studies can be distinguished. **Study A** examines the base cases. The base cases differ in terms of the variable components and whether the curtailment of PPA electricity is prohibited or allowed. The PPAs can always be dimensioned individually in all simulation runs. Three different combinations of optional components with variable size were considered: 1) Only PPAs without additional components; 2) PPAs in combination with a PtH-Steam unit; 3) PPAs in combination with a molten salt TES system. The results of Study A provide information on how much additional renewable electricity a PtH or storage system can integrate into the utility system and what impact this has on the annuity. In addition, the share of curtailment and its impact on the economics can be compared.

Study B is a sensitivity analysis to determine how the optimization results are affected by changes in the price of green hydrogen. Study B focuses on a combination of PPAs with a molten salt TES system. Cases with and without curtailment are considered. The hydrogen price was varied in 10 % increments from 70 % (4.80 €/kg) to 130 % (8.91 €/kg) of the base value. The lower threshold value of the sensitivity analysis represents a progressive hydrogen price with a positive AEL cost trend and lower OPEX than anticipated. In addition, imported green hydrogen could be available at lower cost compared to domestic green hydrogen, provided that the political regulations permit such an option. To put this into perspective, the lower value corresponds approximately to a price forecast for the year 2050 [63]. The higher threshold value, in turn, is a more conservative cost estimate in the event that the AEL cost trend falls short of expectations.

Study C is another sensitivity analysis to investigate the impact of TES investment costs on the optimization results. As in the previous sensitivity analysis, cases with and without curtailment are considered. The investment costs of all three TES components (charge, storage and discharge) are varied in 10 % steps from 70 % to 130 % of the base value (see. Table 1 for base values). The lower end of this parameter variation corresponds to a reduction in TES investment costs due to a positive cost trend or financial support, e.g. government funding. The investment costs derived in this work may underestimate the actual values. The upper threshold of this sensitivity analysis should account for this contingency.

Study D takes a closer look at the impact of steam turbine size. As before, combinations of PPAs with TES and the impact of renewable electricity curtailment are investigated. With larger steam turbine capacities, the potential for electricity generation by the TES system increases. The original steam turbine capacities of the utility system are 30 MW_{el}, 20 MW_{el} and 10 MW_{el} for the high-, medium- and low-pressure steam turbine, respectively. Instead of setting specific fixed values,

Table 4
Overview of conducted optimization runs.

Study A: Base cases			
Acronym	Variable components	Curtailment	H_2 price
PPA-w/oCurt	PV&Wind PPA	x	6.85 €/kg
PtH-w/oCurt	PV&Wind PPA + PtH	x	6.85 €/kg
TES-w/oCurt	PV&Wind PPA + TES	x	6.85 €/kg
PPA-w/Curt	PV&Wind PPA	✓	6.85 €/kg
PtH-w/Curt	PV&Wind PPA + PtH	✓	6.85 €/kg
TES-w/Curt	PV&Wind PPA + TES	✓	6.85 €/kg

Study B: Hydrogen price sensitivity			
Acronym	Variable components	Curtailment	H_2 price
TES-w/oCurt-070%€H2	PV&Wind PPA + TES	x	4.80 €/kg
TES-w/oCurt-080%€H2	"	x	5.48 €/kg
TES-w/oCurt-090%€H2	"	x	6.17 €/kg
TES-w/oCurt-100%€H2	"	x	6.85 €/kg
TES-w/oCurt-110%€H2	"	x	7.54 €/kg
TES-w/oCurt-120%€H2	"	x	8.21 €/kg
TES-w/oCurt-130%€H2	"	x	8.91 €/kg
TES-w/Curt-070%€H2	"	✓	4.80 €/kg
TES-w/Curt-080%€H2	"	✓	5.48 €/kg
TES-w/Curt-090%€H2	"	✓	6.17 €/kg
TES-w/Curt-100%€H2	"	✓	6.85 €/kg
TES-w/Curt-110%€H2	"	✓	7.54 €/kg
TES-w/Curt-120%€H2	"	✓	8.21 €/kg
TES-w/Curt-130%€H2	"	✓	8.91 €/kg

Study C: TES cost sensitivity				
Acronym	Variable components	Curtailment	H_2 price	TES cost
TES-w/oCurt-070%€TES	PV&Wind PPA + TES	x	6.85 €/kg	70 %
TES-w/oCurt-080%€TES	"	x	6.85 €/kg	80 %
TES-w/oCurt-090%€TES	"	x	6.85 €/kg	90 %
TES-w/oCurt-100%€TES	"	x	6.85 €/kg	100 %
TES-w/oCurt-110%€TES	"	x	6.85 €/kg	110 %
TES-w/oCurt-120%€TES	"	x	6.85 €/kg	120 %
TES-w/oCurt-130%€TES	"	x	6.85 €/kg	130 %
TES-w/Curt-070%€TES	"	✓	6.85 €/kg	70 %
TES-w/Curt-080%€TES	"	✓	6.85 €/kg	80 %
TES-w/Curt-090%€TES	"	✓	6.85 €/kg	90 %
TES-w/Curt-100%€TES	"	✓	6.85 €/kg	100 %
TES-w/Curt-110%€TES	"	✓	6.85 €/kg	110 %
TES-w/Curt-120%€TES	"	✓	6.85 €/kg	120 %
TES-w/Curt-130%€TES	"	✓	6.85 €/kg	130 %

Study D: Steam turbine size sensitivity				
Acronym	Variable components	Curtailment	H_2 price	Steam turbines
TES-w/oCurt -ST	PV&Wind PPA + TES	x	6.85 €/kg	81/77/94 MW
TES-w/Curt -ST	"	✓	6.85 €/kg	64/53/65 MW

infinitely large steam turbines were implemented in the utility system to draw conclusions about the optimal capacity. The resulting steam turbine sizes are given in advance in Table 4 to give an idea of how large the components must be to achieve the largest annuity decrease. Since the costs for the steam turbine expansion are not part of the energy system optimization, the results of Study D only provide an indication of whether electricity generation during TES discharge has a noticeable effect on the annuity.

3. Results and discussion

The results are presented in four subsections according to the studies conducted. The base cases are subject of the first subsection (Study A). Then, the sensitivity analysis regarding the hydrogen price is discussed (Study B). After that follow the results of the TES investment cost sensitivity study (Study C). Finally, the influence of steam turbine size on the optimization results is analyzed (Study D).

3.1. Results of Study A: Base cases

The first step is to gain a better understanding of how a PtH unit or TES system can improve the integration of renewable electricity. To this end, Fig. 5 shows the electricity supply and curtailment over a representative period of 48 h for all six base cases. Electricity supply refers to electricity that is transferred to the utility system. Thus, the sum of electricity supply and curtailment equals the maximum renewable electricity generation by PV and wind. For reference, the diagrams include lines for the electricity demand and total energy demand (steam + electricity). The influence of PtH and TES is first explained qualitatively with reference to Fig. 5. The discussion of the quantitative results

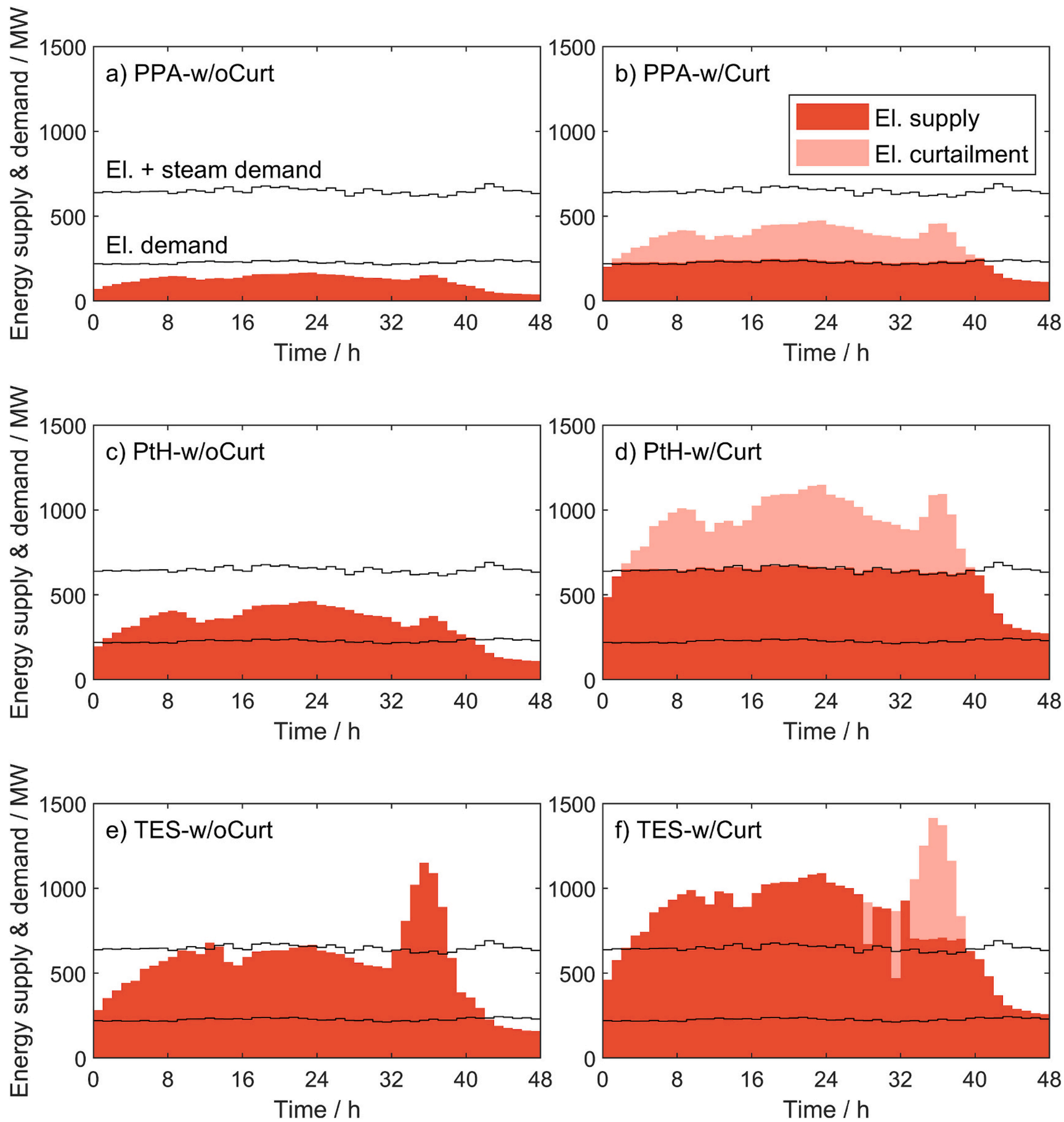

Fig. 5. Electricity supply and curtailment during a two-day period for all base cases.

follows afterwards.

Starting with the two upper diagrams, Fig. 5a (without curtailment) and Fig. 5b (with curtailment) show results for cases in which only PPAs were available as variable components. In these circumstances, the electricity supply cannot exceed the maximum power consumption of the utility system at any time during the year. The maximum power consumption is the sum of the current electricity demand plus the capacity of the small 10 MW_{th} PtH unit. Without curtailment, the electricity feed-in is limited. As can be seen in Fig. 5a, not enough renewable electricity can be supplied to cover the electricity demand in the time period displayed. Allowing curtailment increases electricity procurement, as shown in Fig. 5b. At certain times, the entire electricity demand can be covered by PV and wind. To achieve this, larger volumes of electricity must be curtailed. Apparently, it is economically feasible to bear the cost of curtailment in order to reduce the consumption of expensive green hydrogen. Green hydrogen is still needed to meet parts of the electricity demand and almost the entire steam generation in both cases.

Fig. 5c (without curtailment) and Fig. 5d (with curtailment) show the outcome when the optimizer can build additional PtH-Steam capacity on top of the existing 10 MW_{th} unit. Overall, more renewable electricity can be integrated into the utility system. With a large PtH unit the maximum electricity supply is now limited by the total energy demand. Hence, electricity and steam demand can be partially covered from renewable electricity. As expected, curtailment further improves the electrification of steam production.

Energy storage solutions are required to increase the feed-in of renewable electricity beyond the total energy demand. The optimization results with the TES system as a variable component are presented in Fig. 5e (without curtailment) and Fig. 5f (with curtailment). Electricity procurement is increased compared to the PtH cases. In Fig. 5e, for instance, the electricity supply exceeds the total energy demand between 32 h and 40 h. This surplus electricity is used to charge the TES system. The stored energy can be applied to close gaps between energy demand and renewable energy generation at later times, e.g. between 40 h and 48 h. Curtailment provides flexibility for storage operation to integrate even more renewable electricity, as can be seen in Fig. 5f.

In summary, PtH solutions increase the integration of renewable energy through electric steam generation. TES extends this effect since, in addition to the PtH function, energy can be stored to electrify steam generation and reproduce electricity at times when there is not enough renewable electricity available. Permitting curtailment increases the

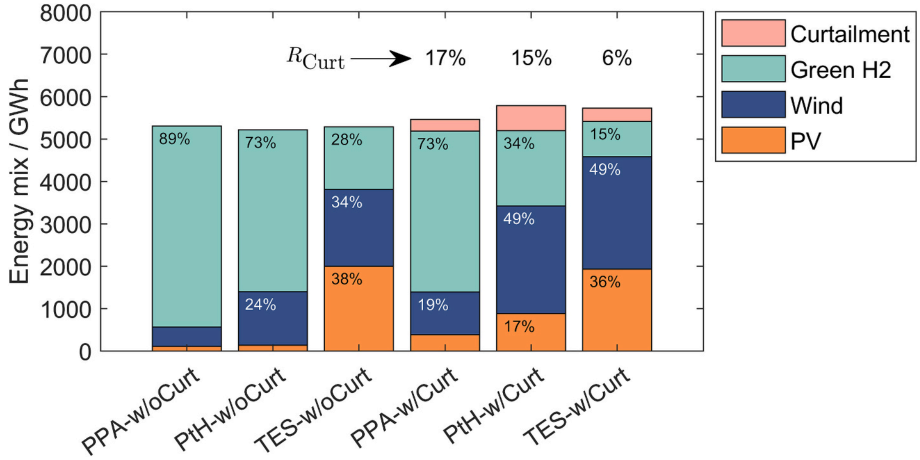

Fig. 6. Breakdown of energy mix and renewable curtailment for all base cases (Share of curtailment in percent values included for all cases where curtailment is permitted; percentage values in the bars show the respective shares of PV, wind and green hydrogen in the energy mix; small contributions are neglected for the purpose of readability). (For interpretation of the references to colour in this figure legend, the reader is referred to the web version of this article.)

feed-in of renewable electricity and the impact of the PtH-Steam and TES system. This additional flexibility in turn enhances the electrification of the energy supply and reduces H_2 consumption.

To put the effects of PtH, TES and curtailment in numbers, Fig. 6 shows the annual energy mix for all six base cases. First of all, minor variations in the overall energy supply can be observed, which can be attributed to different efficiencies of the energy converters. Starting with the PPA only scenario without curtailment, it is evident that the main energy source is green hydrogen, which accounts for 89 % of the energy mix. Renewable electricity is only integrated to a limited extent with an 11 % contribution to the energy mix. In the considered scenario, wind is preferred over PV because it provides more consistent electricity generation (lower variance) over the entire year and is therefore easier to integrate. Additional PtH capacity changes the picture slightly, in that more wind electricity is procured and the share of renewable electricity more than doubles. However, green hydrogen still accounts for the majority of the energy supply. The energy distribution changes significantly with the integration of a TES system. More wind electricity and, in particular, more PV electricity is being integrated. In general, PV electricity has the lowest price and should be integrated first if it is feasible from an operational point of view. The TES system offers the required flexibility to integrate renewable electricity production peaks and handle higher shares of PV electricity. As already discussed, the integration of renewable electricity improves in all cases whenever curtailment is permitted. With TES and by allowing curtailment, renewable electricity accounts for 85 % of the energy mix, while the share of green H_2 drops to 15 %.

The three percentage values above the bars in Fig. 6 with curtailment indicate the share of curtailment. A value of 0 % would indicate that none of the renewable electricity is being curtailed. In the PPA only scenario, 83 % of the potentially available renewable electricity is used and 17 % is curtailed to minimize the annuity. The share of curtailment decreases marginally to 15 % by adding PtH capacity. The deployment of a TES system results in the lowest share of curtailment with 6 %. This demonstrates that TES not only integrates the highest share of renewable electricity and reduces green H_2 consumption, but also results in the most efficient utilization of the PV and wind power plants.

The annuity and its breakdown for the six base cases is depicted in Fig. 7. In principle, a higher share of PV and wind results in lower annuities, as expensive green hydrogen is displaced from the energy supply mix. Large investment sums are required for TES in particular, which are reflected in the annuity. Nonetheless, the cost savings from the reduced procurement of green hydrogen outweigh the investment in TES. Without curtailment, the annuity decreases by 9 % and 22 % with the deployment of a PtH unit or a TES system, respectively. In the case of permissible curtailment, even higher annuity savings can be observed. Here the decrease of annuity amounts to 21 % for the PtH unit and 27 % for the TES system. The difference between PtH and TES is less pronounced with curtailment, since the PtH is capable of integrating larger volumes of low-cost renewable electricity (see Fig. 6).

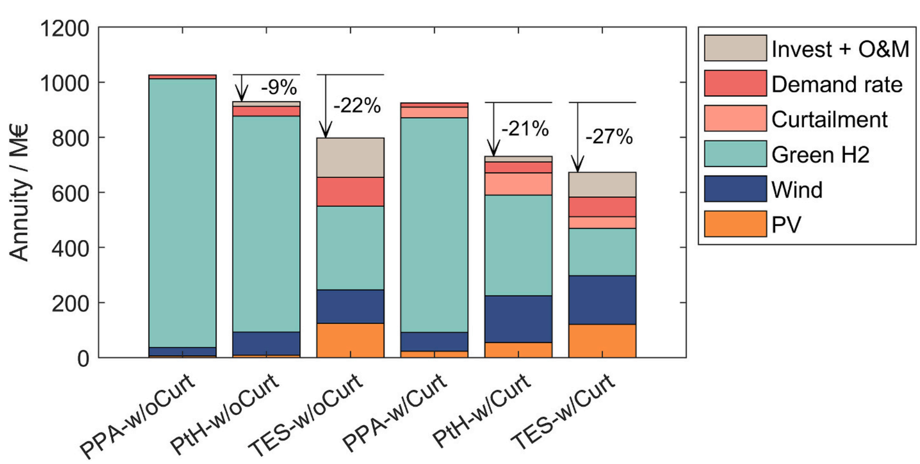

Fig. 7. Breakdown of the annuity for all base cases (Costs for operation & maintenance are included in the annual payment for the investment).

Table 5
Installed capacities of variable components for all base cases.

	PV installed	Wind installed	PtH	TES charge	TES storage	TES discharge
	MW_{el}	MW_{el}	MW_{th}	MW_{th}	MWh_{th}	MW_{th}
PPA-w/oCurt	87	220	–	–	–	–
PtH-w/oCurt	111	608	367	–	–	–
TES-w/oCurt	1604	874	–	1548	11,417	481
PPA-w/Curt	307	623	–	–	–	–
PtH-w/Curt	709	1506	418	–	–	–
TES-w/Curt	1552	1428	–	959	6526	474

In a previous study [27], a similar case with TES was analyzed. However, an energy market scenario based on the European Green Deal was considered. Electricity and gas were procured from the grids and therefore still afflicted with CO_2 emissions. In that study, annual costs (electricity and gas only) were calculated at just over 300 M€ in 2035. In this presented study Fig. 7 shows costs of 510 M€ (sum of PV, wind, H_2 and curtailment bars). Hence, the costs for electricity and gas for zero-emission operation are approximately 210 M€ respectively 70 % higher in the best-case scenario (TES with curtailment) [27].

The installed capacities of all variable components resulting from the optimization are listed in Table 5. The general principles underlying the integration of PV and wind power have already been explained in detail in the previous paragraphs. Table 5 underlines these conclusions by providing the corresponding installed capacities. The size of the PtH and TES discharge units depend on the steam demand and operating conditions. The average and peak steam demands are 362 MW_{th} (see Fig. 1 with 176 MW_{th} + 186 MW_{th}) and 455 MW_{th} (not shown in Fig. 1), respectively. With additional flexibility through curtailment and energy storage, the electrification of steam demand peaks is becoming increasingly economical, leading to larger PtH and TES discharge units. Note that the TES discharge capacity exceeds the maximum steam demand. The reason for this is that additional steam is required to drive the available turbines and generate electricity during discharge.

Without curtailment in particular, very large charging and storage units are required to integrate electricity peaks from PV and wind. These components are sized significantly smaller with permissible curtailment. In addition, the transmission lines to the chemical site can be dimensioned smaller. Hence, curtailment of renewable electricity is more cost-effective than oversizing the TES system and installing additional transmission lines.

3.2. Results of Study B: Hydrogen price sensitivity

The price of green hydrogen is expected to have an impact on the annuity as well as the dimensioning of PPA capacities and the TES system. The annuity breakdown as a function of the green hydrogen price is outlined in Fig. 8. It is only logical that higher green hydrogen prices lead to higher annuities and vice versa. Without curtailment (Fig. 8a), the annuity ranges from −14 % to +12 % compared to the base value with a variation in the green hydrogen price of ±30 %. The share of PV and wind in energy procurement remains rather unaffected, while the cost share of green hydrogen changes with its price. This is an indication that for higher green H_2 prices the feed-in of renewable electricity from PPAs is capped. A combination of PPAs with TES can be efficiently applied up to a certain capacity. The remaining energy demand must be covered by combustion of green hydrogen.

The picture changes again for optimizations with curtailment (Fig. 8b). The improved flexibility allows for more PPA integration and the required amount of green H_2 is smaller compared to the case without curtailment. In fact, the contribution of green H_2 to the annuity is more or less constant, which indicates that less green H_2 is procured at higher prices. The reduction in green H_2 consumption is compensated by the integration of more wind power, while the cost and energy share of PV remains unaffected by the price of green H_2. In the case with curtailment, the annuity variation is smaller with −10 % to +6 % compared to the base value with a variation in the green hydrogen price of ±30 %. Slightly more renewable electricity is curtailed towards higher green H_2 prices. The share of curtailment ranges from 4 % (70 % green H_2 price) to 8 % (130 % green H_2 price).

Fig. 9 gives more insight into the influence of the green hydrogen price on the energy mix and TES unit sizes.

Fig. 9a shows that without curtailment the **share of green H_2 in the energy mix** can only be reduced to a small extent. In particular towards higher green hydrogen prices almost no reduction occurs. By allowing curtailment the share of green hydrogen decreases significantly from 23 % to 11 % over the considered price range. As already discussed, this is achieved by integrating more **PV** (Fig. 9b) and **wind** (Fig. 9c) electricity into the utility system. A modest increase in the share of PV electricity can be observed for both cases without and with curtailment. Even with curtailment allowed, there is apparently an upper limit for PV PPAs that can be economically integrated. With curtailment green hydrogen is largely substituted by wind electricity.

The **TES charge power** (Fig. 9d) increases moderately for cases without curtailment to be capable of utilizing the added PV electricity. Interestingly, with curtailment the TES charge power hardly changes despite of a substantial increase in wind PPAs. The higher electricity peaks are handled by expanding curtailment at higher green H_2 prices (see discussion of Fig. 8). With this measure, a small increase of TES charge power apparently suffices to integrate the majority of the additional wind electricity.

The influence of the green H_2 price on the **TES capacity** is shown in Fig. 9e. The TES capacity increases for both cases with and without curtailment. For higher H_2 prices, larger sized TES systems can store more renewable electricity. In the case without curtailment, in general larger storage units are required because renewable electricity peaks must be stored by the TES system. The increase flattens towards higher green H_2 prices, as the feed-in of renewable electricity is capped (see Fig. 9b and Fig. 9c). In the case with curtailment the TES capacity more than doubles from 4 GWh_{th} to over 9 GWh_{th} in the considered green hydrogen price range of ±30 %. As discussed before, very large production peaks are addressed by curtailment, to keep the cost of the expensive TES charge unit at a minimum. However, an increase in storage capacity is required to store the overall higher wind electricity supply (see Fig. 9c).

Finally, the **TES discharge power** is plotted over the green hydrogen price in Fig. 9f. The size of the TES discharge unit is almost independent of the green hydrogen price or how curtailment is handled. As already mentioned, steam demand and feasible full load hours are the decisive influencing factors. With and without curtailment, a small increase of the TES discharge power can be observed. During discharge of the TES system, electricity generation with the on-site steam turbines becomes more attractive at higher green H_2 prices, which in turn leads to slightly larger discharge units.

3.3. Results of Study C: TES cost sensitivity

Similar to the price of green hydrogen, the investment costs for TES should also have a considerable influence on the optimal utility system.

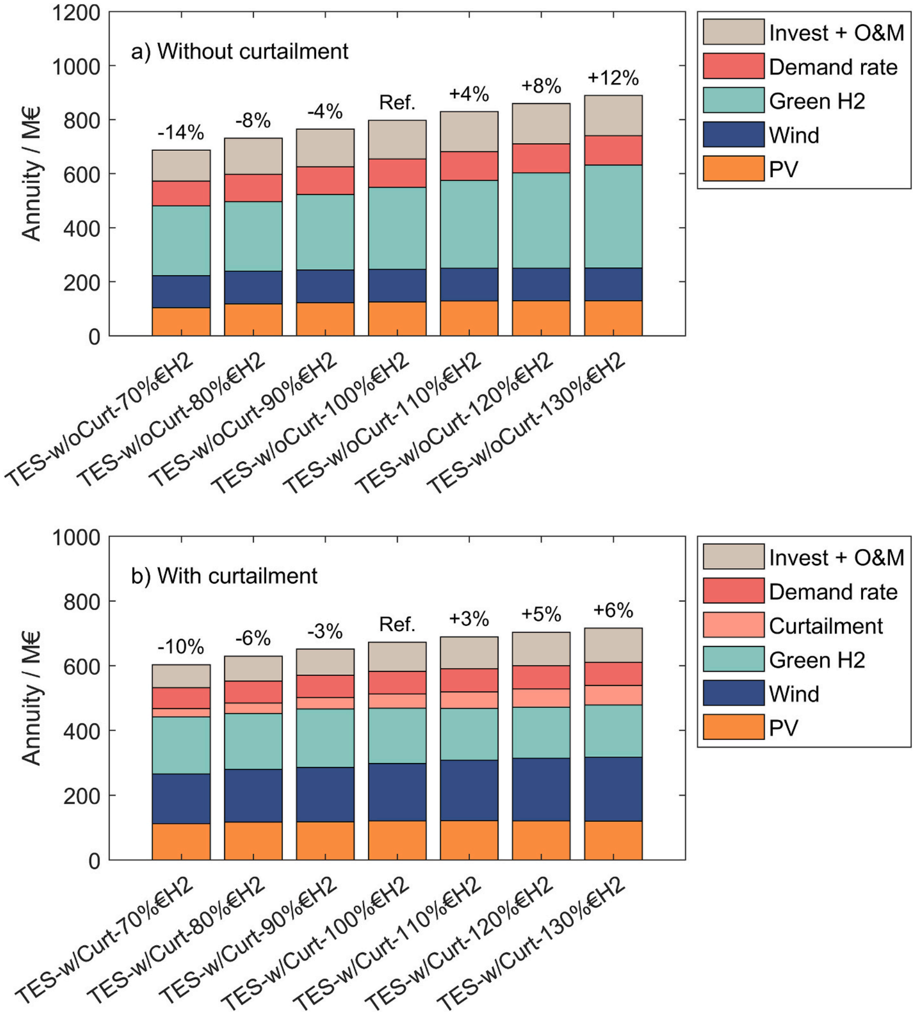

Fig. 8. Breakdown of the annuity depending on the green hydrogen price a) without curtailment and b) with curtailment. (For interpretation of the references to colour in this figure legend, the reader is referred to the web version of this article.)

First, the breakdown of the energy mix in relation to the TES investment costs is depicted in Fig. 10. Without curtailment (Fig. 10a), the influence on the energy mix appears to be rather negligible. Within the investigated TES cost range, the share of renewable electricity in the energy mix varies between 73 % at the lower to 71 % at the upper threshold of the sensitivity analysis. The influence of the TES costs is slightly more pronounced for cases with curtailment (Fig. 10b). The share of renewable electricity in the energy mix changes from 87 % to 83 % over the TES cost range. As the costs of TES decrease, more renewable PPAs are integrated to substitute green hydrogen and vice versa. The share of curtailment is more or less constant in all cases investigated and lies between 6 % and 7 %.

Fig. 11 shows the results of the sensitivity study with respect to the annuity. Considering the cases without curtailment first (Fig. 11a), the annuity varies from −6 % to +5 % within the given TES cost range. With the exception of investment as well as O&M costs, the annuity contributions are relatively constant. This is to be expected, as the energy mix is not influenced by the cost of TES either. In fact, the costs also have a limited influence on the size of the storage components. The storage capacity, for instance, decreases from 12.1 GWh (−30 % TES costs) to 10.7 GWh (+30 % TES costs) when curtailment is not allowed.

The impact on the annuity is even smaller for optimizations with curtailment (Fig. 11b). Here, the annuity ranges from −4 % to +3 % compared to the base value within the TES investment costs spread of ±30 %. There are only marginal changes in the contribution of investment and O&M costs to the annuity. In conclusion, the size of the storage components changes significantly for cases with curtailment. Here, the storage capacity decreases from 10.5 GWh (−30 % TES costs) to 4.7 GWh (+30 % TES costs). Apparently, as the investment costs for TES increase, it becomes more favorable to enhance renewable electricity integration by curtailment.

In general, the results of the TES cost sensitivity study are similar to those of the previous analysis of the green hydrogen price. Without curtailment, flexibility in optimization is more limited and the ideal composition of green hydrogen, PPAs and thermal energy storage is subject to tighter restrictions. With curtailment, PPAs and TES systems can be dimensioned more independently. Overall, the impact of the TES investment costs appears to be smaller compared to the green hydrogen price. This can be attributed to the fact that storage costs generally make up a smaller contribution to the annuity.

3.4. Results of Study D: Steam turbine size sensitivity

The electricity generation capacity during TES discharge depends, inter alia, on the available steam turbines (Fig. 1). In this sensitivity study, infinitely large steam turbines were available for energy system optimization to determine the maximum effect of larger steam turbines on the annuity. A cost analysis and optimization of the additional steam

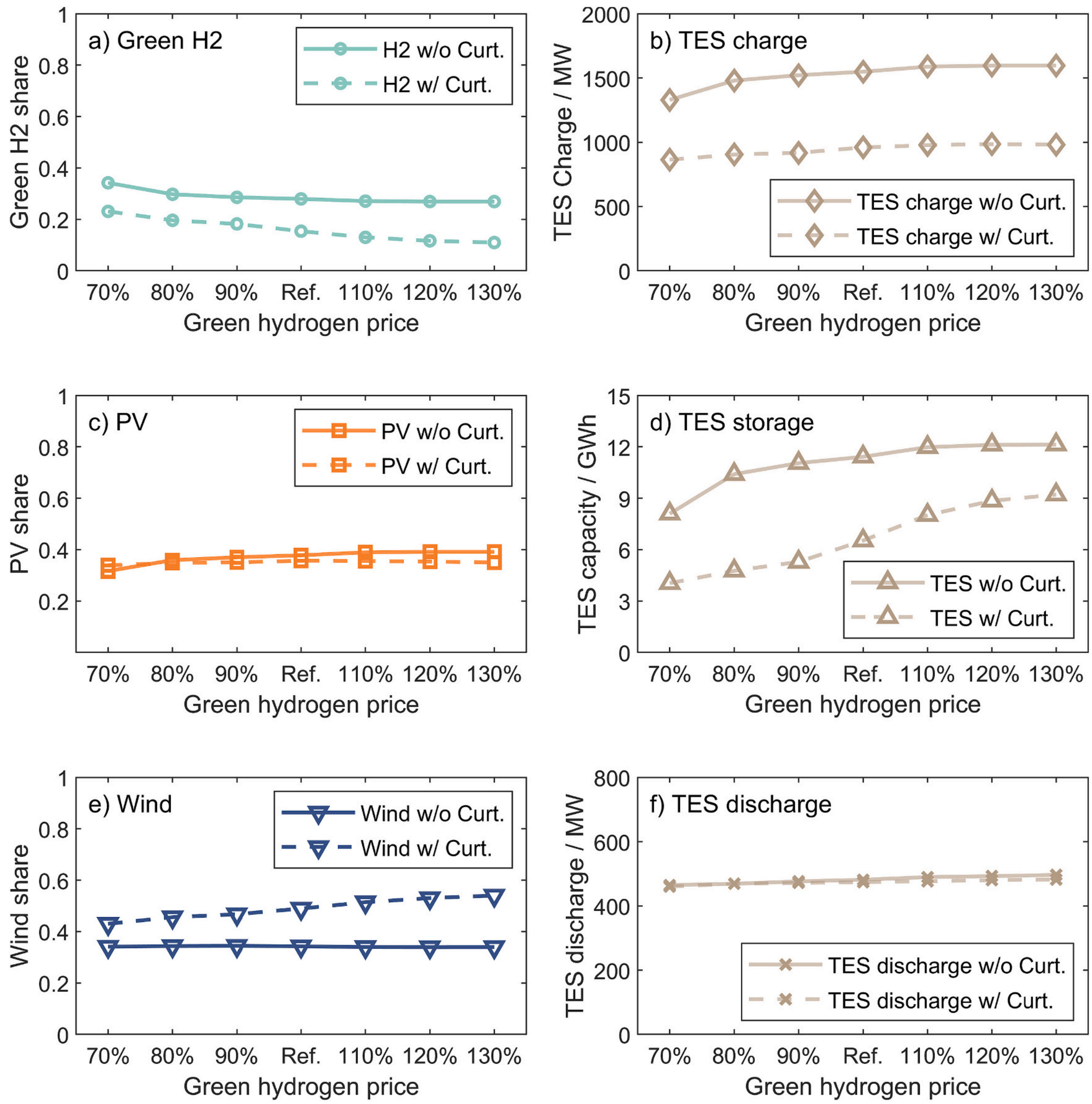

Fig. 9. Influence of the green hydrogen price on a) share of green hydrogen supply, b) TES charge power, c) share of PV electricity, d) TES storage capacity, e) share of wind electricity and f) TES discharge power. (For interpretation of the references to colour in this figure legend, the reader is referred to the web version of this article.)

turbine power was not carried out.

The results for the annuity are shown in Fig. 12. The cases with larger steam turbines are compared with the corresponding base cases. The same green hydrogen price and PPAs + TES were considered as variable components. Without curtailment, the annuity can be reduced by 5 %. With the added flexibility of larger steam turbines, it becomes more economical to integrate larger volumes of wind electricity to substitute green hydrogen. The same applies to some extent to the case with curtailment. However, the annuity reduction amounts to only 1 %.

To provide a better view on the results of this study, Table 6 lists the installed PPA capacities as well as the TES component and steam turbine sizes for the cases under consideration. In the standard case the steam turbine capacities are 30 MW_{el}, 20 MW_{el} and 10 MW_{el} (see Fig. 1) The values provided for the new cases with infinite steam turbine capacities represent the maximum output determined by the optimizer within the representative year. Especially when curtailment is prohibited, a significant increase of PPA capacities, in particular wind, can be observed. To account for this a larger TES charge unit is installed. Contrary to expectations, the size of the TES storage unit is reduced.

Apparently, it is feasible to charge and discharge the TES system more frequently if larger steam turbines are available. This can also be seen from the ratio between TES charging and discharging power (without curtailment and with standard steam turbines 1548 MW_{th} / 481 MW_{th} = 3.2; without curtailment and with larger steam turbines 1924 MW_{th} / 1005 MW_{th} = 1.9). A ratio of 1 means only PtH mode of the TES system while larger ratios correspond to increasing storage periods (see subsection 2.1). For larger steam turbines, the TES discharge unit is sized up significantly to produce enough steam to drive the on-site turbines. To achieve the 5 % annuity reduction, the steam turbines must be significantly larger. For example, for the case without curtailment, the maximum power of the low-pressure steam turbine must be increased more than ninefold.

Similar observations can be made for the case with curtailment. However, the increase of PPAs, TES system and steam turbines is less pronounced. The ratio between charge and discharge power decreases from 2.0 to 1.4 when larger steam turbines are available. The annuity can only be reduced by 1 % with larger steam turbines compared to the base case.

Despite significantly larger steam turbines, the annuity cannot be reduced by >5 % and 1 % without or with curtailment, respectively.

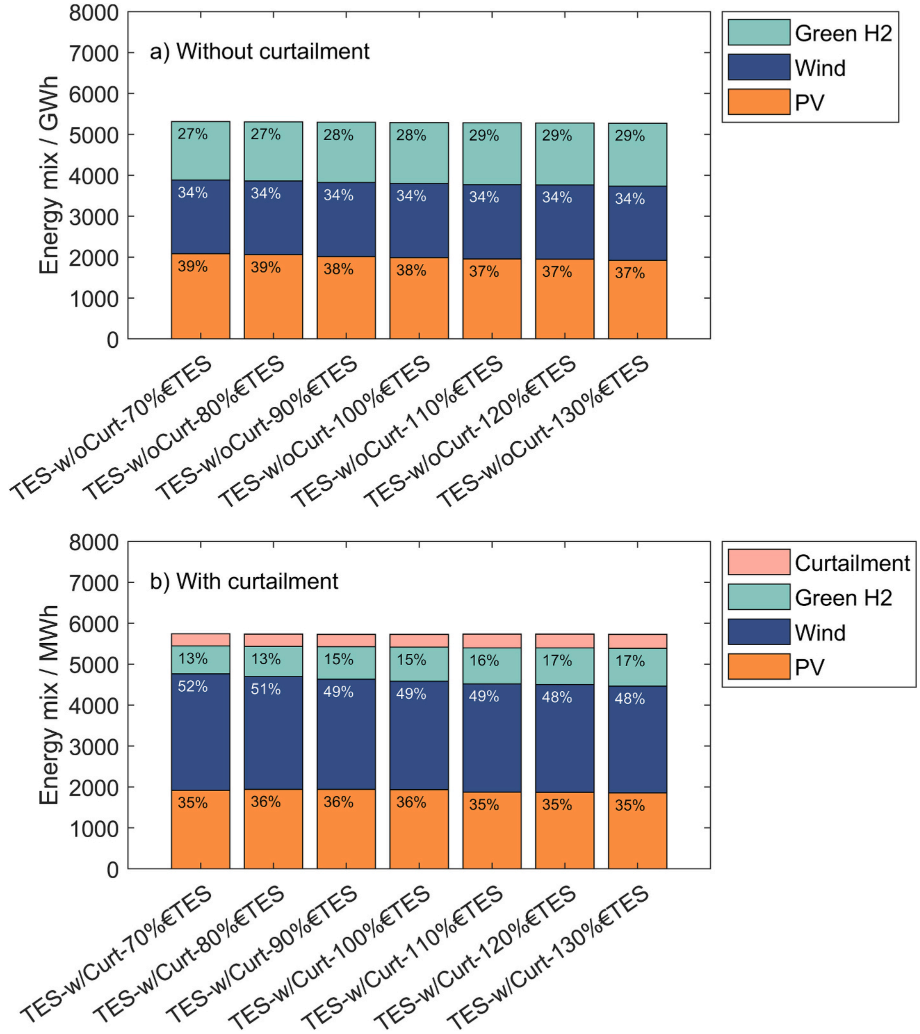

Fig. 10. Breakdown of the energy mix depending on the TES investment costs a) without curtailment and b) with curtailment (percentage values in the bars show the respective shares of PV, wind and green hydrogen in the energy mix). (For interpretation of the references to colour in this figure legend, the reader is referred to the web version of this article.)

There are two reasons for this: 1) Due to the PPA contracts with large installed PV and wind capacities, hours with an undersupply of electricity are uncommon. For instance, in the case with curtailment and standard steam turbine sizes, there are roughly 2000 h per year with an undersupply of renewable electricity. As a result, the operating hours of the steam turbines are generally limited. 2) High quantities of steam are required to drive these large steam turbines. Ideally, the steam is transferred between the steam lines via the turbines and then used to meet demand for maximum efficiency. Excess steam that cannot be fed to the end-use processes must be passed through the low-pressure steam turbine and condensed in a cooling tower. This leads to a reduction in the overall system efficiency. This efficiency reduction in turn is predicted to limit the economic impact of larger steam turbines.

Although extending the turbine capacity results in a lower overall annuity of −5 % without curtailment and − 1 % with curtailment, it is questionable whether this option is of interest to utility system operators. Annuity savings are small compared to the investments in steam turbines and a larger TES. Such large steam turbines are not typically available since utility systems are primarily steam producers and use the steam turbines in addition for arbitrage trades on the electricity market. Finally, the space required for large cooling towers can be a showstopper, as the available space in chemical sites may not be available.

4. Summary and conclusion

This paper addressed the concept of a zero-emission utility system at a typical large German chemical site. PV and wind power purchase agreements (PPAs) as well as green hydrogen were considered as CO_2-free energy carriers. The flexibility options investigated included the curtailment of renewable energy, power-to-heat (PtH) and thermal energy storage (TES). A model of a zero-emission utility system was developed. The required input data were compiled, consisting of PPA prices and generation profiles, curtailment cost, green hydrogen price and the investment costs of PtH and TES components. Transmission lines from power plants to the utility system as well as H_2 pipelines were not considered as investment costs in this study. The model was implemented in TOP-Energy® for combined operational and structural optimization. The size of the following components was optimized: Installed capacities of PV and wind power plants corresponding to PPAs, PtH-Steam, TES charging unit, TES capacity, and TES discharging unit.

In general, the feed-in of renewable electricity to **substitute expensive green hydrogen** is the key pathway to reduce annual expenditures. If the **curtailment of renewable electricity** is not permitted, the feed-in of PV electricity in the chemical site is heavily restricted. PV and wind power supply cannot exceed the maximum

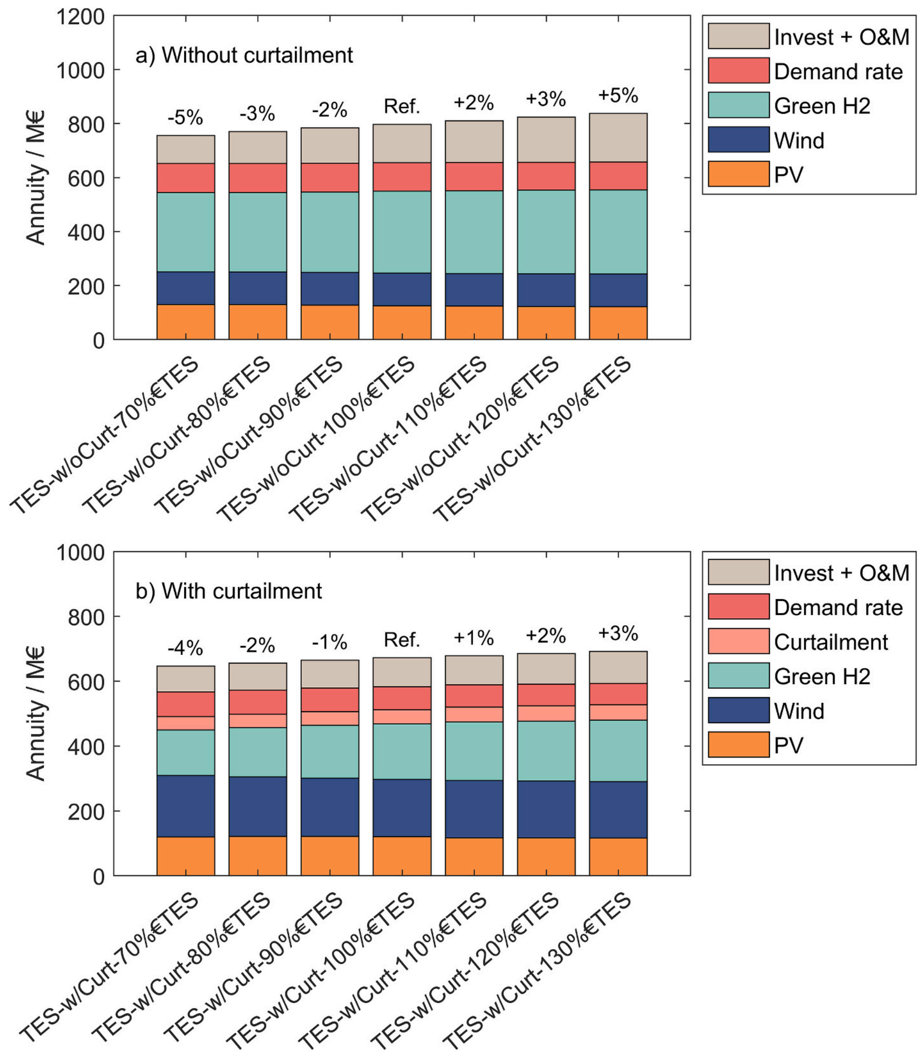

Fig. 11. Breakdown of the annuity depending on the TES investment cost a) without curtailment and b) with curtailment.

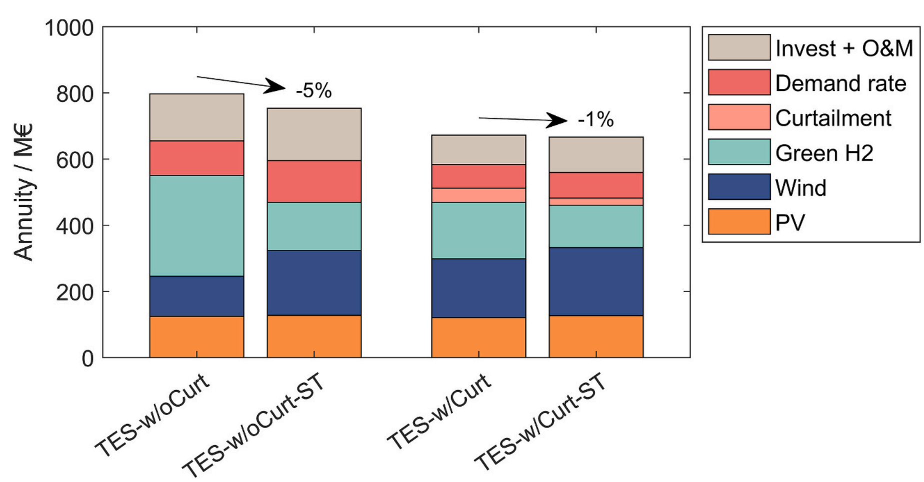

Fig. 12. Breakdown of the annuity for the steam turbine size sensitivity compared to the corresponding base cases.

electricity consumption of the utility system at any time of the year. By adding a PtH unit, the feed-in of renewable electricity can be increased to the combined electricity and steam demand. By implementing a TES system, the renewable electricity feed-in can exceed the aforementioned limitations. The TES system achieves this with two operating modes: 1) PtH mode: Direct steam production from renewable electricity without a time shift; 2) Charge and discharge mode: Surplus electricity is stored and used at a later time when less renewable electricity is available.

The results for the case **without curtailment** regarding the energy supply with green hydrogen and renewable electricity are as follows:

Table 6
Installed capacities of flexible components and steam turbines for the steam turbine sensitivity study in comparison to the equivalent base bases.

	PV installed	Wind installed	TES charge	TES torage	TES discharge	Steam turbines*
	MW_{el}	MW_{el}	MW_{th}	MWh_{th}	MW_{th}	MW_{el}
TES-w/oCurt	1604	874	1548	11,417	481	30/20/10
TES-w/oCurt-ST	1648	1415	1924	8848	1005	81/77/94
TES-w/Curt	1552	1428	959	6526	474	30/20/10
TES-w/Curt-ST	1630	1559	1055	7717	774	64/53/65

* The column steam turbine shows the installed capacity of the HP-, MP- and LP-ST in that order.

- Only PPAs available: 89 % green H_2 and 11 % electricity
- PPAs + PtH-Steam: 73 % green H_2 and 27 % electricity
- PPAs + TES system: 28 % green H_2 and 72 % electricity

Allowing **curtailment** improves the operational flexibility of the utility system. This leads to higher electrification rates, which reduces the required amount of expensive green hydrogen and consequently the annuity. The energy supply with green hydrogen and renewable electricity in the cases **with curtailment** is outlined below. The share of curtailment is given as additional information:

- Only PPAs available: 73 % H_2 and 27 % Electricity
  (Share of curtailment 17 %)
- PPAs + PtH-Steam: 34 % H_2 and 66 % Electricity
  (Share of curtailment 15 %)
- PPAs + TES system: 15 % H_2 and 85 % Electricity
  (Share of curtailment 6 %)

Although the impact of TES is less profound when curtailment is allowed, TES does lead to the lowest curtailment rate of 6 %. This means that the deployment of TES results in the lowest annuities and highest electrification rate, while the PV and wind installations are well utilized and minimal renewable electricity is curtailed.

A **sensitivity analysis** was carried out with respect to the **green hydrogen price** to further expand the scope of the study. The green hydrogen price was varied by ±30 % of the base value and cases with TES were considered. Within the specified hydrogen price range, the annuity changes from −14 % to +12 % without curtailment allowed. The impact of the green hydrogen price variation is less significant with permissible curtailment. In this case, the annuity varies only from −10 % to +6 % compared to the base case. This sensitivity study provided further evidence that very large TES systems are required to integrate PV and wind electricity if curtailment is not allowed. Furthermore, there appears to be a threshold for the maximum renewable electrification. Beyond this point, it is more cost-effective to combust green hydrogen rather than building even larger TES components in combination with an extension of PPAs. On the other hand, the share of green hydrogen can be reduced significantly and cost-effectively, if curtailment is permitted. This is achieved by increasing the share of PPA electricity and the increase of TES storage capacity. In this way, more renewable energy is integrated while generation peaks are tackled through curtailment.

The second **sensitivity analysis** looked into the influence of **TES investment costs** on the energy mix and annuity. The TES investment costs were varied by ±30 % of the base value. The annuity changes from −6 % to +5 % without curtailment allowed. With curtailment, the impact of TES costs is further reduced. Here the annuity varies from −4 % to +3 % within the investigated cost range. Overall, the annuity is less affected compared to the hydrogen price variation. This is due to the fact that investment and O&M have a smaller cost contribution compared to green hydrogen. The main conclusions of this sensitivity are as follows. Without curtailment, the renewable electricity integration appears to be capped. However, despite higher investment costs, it is still economically feasible to build large TES systems rather than switching to a higher share of green hydrogen. If curtailment is permissible, the TES systems are dimensioned significantly smaller with increasing investment costs. However, the share of PV and wind electricity in the energy mix still increases in this case, since production peaks can be curtailed for a fee. One of the most important findings is that TES is always a core component of the optimal zero-emission utility system, even with very high investment cost assumptions.

Finally, the influence of the on-site **steam turbine sizes** and thus the potential for electricity generation by the TES system during discharge was studied. The electricity demand is already well covered by the PPAs, resulting in low operating hours of the steam turbines. In addition, large volumes of steam are required to ramp up the turbines. Steam that exceeds the demand must be processed through the low-pressure turbine and then condensed. This leads to a reduction in the overall efficiency of the system which also affects the economics. In summary, it can be stated that larger steam turbines do not result in a notable reduction of the annuity and a substantial increase in steam turbine power does not appear to be a viable option.

In conclusion, this paper has shown that a zero-emission utility system is feasible within the next decade, albeit requiring substantial investments in green H_2, electricity grid extensions, as well as flexibility options. As flexibility options, TES plays a crucial role and shows the best performance for efficient electrification and thus low annual expenditures. Allowing curtailment of electricity from renewables can further enhance the impact of TES and reduces electricity transmission line installations. It is recommended to allow sufficient lead time for the implementation of a zero-emission utility system for a chemical site. Topics relevant for the adaptation of the utility system are: Clarification of the regulatory framework; creation of a roadmap; expansion of the electricity and hydrogen grid; development of test installations; approval process; implementation and commissioning of the utility system adaptation with TES.

CRediT authorship contribution statement

Marco Prenzel: Writing – original draft, Visualization, Validation, Methodology, Investigation, Formal analysis, Data curation, Conceptualization. **Freerk Klasing:** Writing – review & editing, Methodology. **Stefan Kirschbaum:** Writing – review & editing, Software, Funding acquisition. **Thomas Bauer:** Writing – review & editing, Supervision, Project administration, Funding acquisition.

Declaration of competing interest

The authors declare that they have no known competing financial interests or personal relationships that could have appeared to influence the work reported in this paper.

Acknowledgements

The authors thank the German Federal Ministry for Economic Affairs and Climate Action (BMWK) for the financial support given to this work in the project TransTES-Chem 03ET1646A-E.

We are also grateful for the valuable discussions with and feedback from Karen Perrey (Covestro AG) and Juliane Trautmann (TSK Flagsol) in the course of this publication.

Data availability

The TOP-Energy® model of the zero-emission utility system (as used in this work), including all necessary input parameters as well as the result data, can be provided by the first author on request.

References

[1] Boehm, S., L. Jeffery, et al., *State of Climate Action* 2023. 2023, Bezos Earth Fund, Climate Action Tracker, Climate Analytics, ClimateWorks Foundation, NewClimate Institute, the United Nations Climate Change High-Level Champions, and World Resources Institute: Berlin and Cologne, Germany, San Francisco, CA, and Washington, DC. https://doi.org/10.46830/wrirpt.23.00010.

[2] United Nations. *Paris Agreement*. [Last accessed on Dec. 18, 2024]. Available from: https://unfccc.int/sites/default/files/english_paris_agreement.pdf.

[3] Scheuermann, A. *Chemical industry tackles biggest transformation in its history*. [Last accessed on Dec. 18, 2024]. Available from: https://www.achema.de/en/press/trend-reports/chemical-industry-tackles-biggest-transformation-in-its-history.

[4] Covestro AG. *Climate Neutrality 2035*. [Last accessed on Dec. 18, 2024]. Available from: https://www.covestro.com/en/sustainability/what-drives-us/climate-neutrality.

[5] GHG Protocol. *FAQ*. [Last accessed on Dec. 18, 2024]. Available from: https://ghgprotocol.org/sites/default/files/standards_supporting/FAQ.pdf.

[6] T. Bernoville. What are Scopes 1, 2 and 3 of Carbon Emissions? [Last accessed on Dec. 18, 2024]. Available from: https://plana.earth/academy/what-are-scope-1-2-3-emissions#explained-scope-1-2-and-3-emissions.

[7] United Nations Industrial Development Organization. *Manual for Industrial Steam Systems Assessment and Optimization*. [Last accessed on Dec. 18, 2024]. Available from: https://www.unido.org/sites/default/files/2017-11/SSO-Manual-Print-FINAL-20161109-One-Page-V2.pdf.

[8] S. Madeddu, F. Ueckerdt, et al., The CO2 reduction potential for the European industry via direct electrification of heat supply (power-to-heat), Environ. Res. Lett. 15 (12) (2020) 124004, https://doi.org/10.1088/1748-9326/abbd02.

[9] S. Lechtenböhmer, L.J. Nilsson, et al., Decarbonising the energy intensive basic materials industry through electrification – Implications for future EU electricity demand, Energy 115 (2016) 1623–1631, https://doi.org/10.1016/j.energy.2016.07.110.

[10] A. Otto, M. Robinius, et al., Power-to-steel: Reducing CO2 through the integration of renewable Energy and Hydrogen into the German steel industry, Energies 10 (2017), https://doi.org/10.3390/en10040451.

[11] E. Palm, L.J. Nilsson, M. Åhman, Electricity-based plastics and their potential demand for electricity and carbon dioxide, J. Clean. Prod. 129 (2016) 548–555, https://doi.org/10.1016/j.jclepro.2016.03.158.

[12] A. Hasanbeigi, M.J.S. Zuberi, Electrification of Steam and Thermal Oil Boilers in the Textile Industry: Techno-Economic Analysis for China, Japan, and Taiwan, Energies 15 (2022), https://doi.org/10.3390/en15239179.

[13] M.J.S. Zuberi, A. Hasanbeigi, W. Morrow, Electrification of industrial boilers in the USA: potentials, challenges, and policy implications, Energ. Effic. (2022) 15, https://doi.org/10.1007/s12053-022-10079-0.

[14] M. Wei, C.A. McMillan, S. de la Rue du Can, Electrification of industry: Potential, challenges and outlook, Electrification 6 (2019) 140–148, https://doi.org/10.1007/s40518-019-00136-1.

[15] E. Sandberg, A. Toffolo, A. Krook-Riekkola, A bottom-up study of biomass and electricity use in a fossil free Swedish industry, Energy 167 (2019) 1019–1030, https://doi.org/10.1016/j.energy.2018.11.065.

[16] R. Adam, B. Ozarisoy, Techno-economic analysis of state-of-the-art carbon capture Technologies and their applications, Scient Metric Review Encyclopedia 3 (2023) 1270–1305, https://doi.org/10.3390/encyclopedia3040092.

[17] G. Lu, Z. Wang, et al., Recent progress in carbon dioxide capture technologies: A review, Clean Energy Sci. Technol. (2023) 1, https://doi.org/10.18686/cest.v1i1.32.

[18] A. Hörbe Emanuelsson, F. Johnsson, The cost to consumers of carbon capture and storage—a product value chain analysis, Energies 16 (7113) (2023), https://doi.org/10.3390/en16207113.

[19] O.A. Ibigbami, O.D. Onilearo, R.O. Akinyeye, Post-combustion capture and other carbon capture and sequestration (CCS) technologies: A review, Environ. Qual. Manag. (2024), https://doi.org/10.1002/tqem.22180.

[20] C. Hepburn, E. Adlen, et al., The technological and economic prospects for CO2 utilization and removal, Nature 575 (7781) (2019) 87–97, https://doi.org/10.1038/s41586-019-1681-6.

[21] General Electric. *Hydrogen Overview*. [Last accessed on Dec. 18, 2024]. Available from: https://www.gevernova.com/content/dam/gepower-new/global/en_US/downloads/gas-new-site/future-of-energy/hydrogen-overview.pdf.

[22] Siemens Energy. *Wasserstoff-Perspektive für Gaskraftwerke wird konkret*. [Last accessed on Dec. 18, 2024]. Available from: https://www.siemens-energy.com/de/de/home/pressemitteilungen/wasserstoff-perspektive-fuer-gaskraftwerke-wird-konkret.html.

[23] The Babcock & Wilcox Company. *BrightGen™ Hydrogen Combustion Technology - Utilizing non-carbon-based fuels for steam production*. [Last accessed on Dec. 18, 2024]. Available from: https://www.babcock.com/assets/PDF-Downloads/PS-599-BrightGen-Hydrogen-Combustion-Brochure.pdf.

[24] Hydrogen Technologies LLC. *Dynamic Combustion Chamber*. [Last accessed on Dec. 18, 2024]. Available from: https://hydrogentechnologiesllc.com/wp-content/uploads/sites/2/2023/04/HT_Report_DynamicCombustionChamber-2023.pdf.

[25] G. Backofen, J. Haimerl, et al., Thermochemical Energy Storage for Increasing the Flexibility of an Industrial Combined Heat and Power Plant, 34th International Conference on Efficiency, Cost, Optimization, Simulation and Environment Impact of Energy Systems (ECOS 2021), Taormina, Italy, https://doi.org/10.52202/062738-0095.

[26] G. Backofen, M. Würth, et al., Power-to-Process-Heat in Industrial Combined Heat and Power Plants – Integration of a Large-Scale Thermochemical Energy Storage, Atlantis Highlights in Engineering (2022), Proceedings of the International Renewable Energy Storage Conference 2021 (IRES 2021), https://doi.org/10.2991/ahe.k.220301.002.

[27] M. Prenzel, F. Klasing, et al., The Potential of Thermal Energy Storage for Sustainable Energy Supply at Chemical Sites, Atlantis Highlights in Engineering (2023), Proceedings of the International Renewable Energy Storage Conference (IRES 2022), https://doi.org/10.2991/978-94-6463-156-2_25.

[28] C. Reinert, N. Nolzen, et al., Design of low-carbon multi-energy systems in the SecMOD framework by combining MILP optimization and life-cycle assessment, Comput. Chem. Eng. 172 (2023) 108176, https://doi.org/10.1016/j.compchemeng.2023.108176.

[29] D. Atabay, An open-source model for optimal design and operation of industrial energy systems, Energy 121 (2017) 803–821, https://doi.org/10.1016/j.energy.2017.01.030.

[30] P. Bartsch, S. Zunft, Kapitel 3: Thermische Speicher, in: F. Ausfelder, S. von Roon, A. Seitz (Eds.), Flexibilitätsoptionen in der Grundstoffindustrie II Analysen | Technologien | Beispiele, 2019. Available from: https://dechema.de/dechema_media/Downloads/Positionspapiere/2019_Kopernikus_Flexoptionen_Band+II_kompl.pdf.

[31] O. Garbrecht, M. Bieber, R. Kneer, Increasing fossil power plant flexibility by integrating molten-salt thermal storage, Energy 118 (2017) 876–883, https://doi.org/10.1016/j.energy.2016.10.108.

[32] N. Nolzen, L. Leenders, A. Bardow, Flexibility-expansion planning of multi-energy systems by energy storage for participating in balancing-power markets, Frontiers in Energy Research (2023) 11, https://doi.org/10.3389/fenrg.2023.1225564.

[33] F. Klasing, C. Odenthal, T. Bauer, Assessment for the adaptation of industrial combined heat and power for chemical parks towards renewable energy integration using high-temperature TES, Energy Procedia 155 (2018) 492–502, https://doi.org/10.1016/j.egypro.2018.11.031.

[34] T. Bauer, C. Odenthal, A. Bonk, Molten salt storage for power generation, Chemie Ingenieur Technik 93 (4) (2021) 534–546, https://doi.org/10.1002/cite.202000137.

[35] T. Bauer, N. Breidenbach, et al., Overview of molten salt storage systems and material development for solar thermal power plants, in: World Renewable Energy Forum, 2012. Available from: https://www.proceedings.com/15138.html. Denver, Colorado, United States.

[36] Neoen. *Victorian Big Battery*. [Last accessed on December 18, 2024]. Available from: https://victorianbigbattery.com.au/.

[37] Cole, W. and A. Karmakar, *Cost Projections for Utility-Scale Battery Storage:* 2023 *Update*. 2023, National Renewable Energy Laboratory (NREL): Golden, Colorado, United States. Available from: https://www.nrel.gov/docs/fy23osti/85332.pdf.

[38] T. Bauer, M. Prenzel, et al., Ideal-typical utility infrastructure at chemical sites – definition, operation and Defossilization, Chem. Ing. Tech. 94 (6) (2022), https://doi.org/10.1002/cite.202100164.

[39] F. Ausfelder, C. Beilmann, et al., Energy storage as part of a secure Energy supply, Chem. Ing. Tech. 87 (1–2) (2015) 17–89, https://doi.org/10.1002/cite.201400183.

[40] STEAG Energy Services GmbH. *EBSILON®Professional 15.02*. [Last accessed on Dec. 18, 2024]. Available from: https://www.ebsilon.com/uploads/pics/Release_15_Notes_en_2020_01.pdf.

[41] Deutscher Wetterdienst. *Testreferenzjahre (TRY)*. [Last accessed on Dec. 18, 2024]. Available from: https://www.dwd.de/DE/leistungen/testreferenzjahre/testreferenzjahre.html.

[42] J. Theis, Quality Guidelines for Energy Systems Studies: Cost Estimation Methodology for NETL Assessments of Power Plant Performance, 2021. United States, https://doi.org/10.2172/1567736.

[43] International Energy Agency (IEA), The Future of Hydrogen - Seizing today's opportunities, 2019. Paris, Available from: https://www.iea.org/reports/the-future -of-hydrogen.

[44] R. Große, C. Binder, et al., Long Term (2050) Projections of Techno-Economic Performance of Large- Scale Heating and Cooling in the EU, European Union, 2017, https://doi.org/10.2760/24422.

[45] T. Drees, H. Medert, et al., Netzentwicklungsplan Strom 2035, Version 2021, 2. Entwurf - Kostenschätzungen, 2021. Available from: https://www.netzentwicklungsplan.de/sites/default/files/2023-02/26_NEP_2035_V2021_2E_Kostenschaetzung_0.pdf.

[46] M. Du, Y. Zhao, et al., Lifecycle cost forecast of 110 kV power transformers based on support vector regression and gray wolf optimization, Alex. Eng. J. 60 (6) (2021) 5393–5399, https://doi.org/10.1016/j.aej.2021.04.019.

[47] F. Trieb, J. Jäger, et al., Thermal storage power plants – key for transition to 100% renewable energy, Journal of Energy Storage 74 (2023) 109275, https://doi.org/10.1016/j.est.2023.109275.

[48] J. Iñigo-Labairu, J. Dersch, L., Schomaker integration of CSP and PV power plants: investigations about synergies by close coupling, Energies 15 (2022), https://doi.org/10.3390/en15197103.

[49] J. Dersch, J. Paucar, et al., Blueprint for Molten Salt CSP Power Plant, Cologne, Germany. Final report of the research project "CSP-Reference Power Plant" No. 0324253 (2021). Available from: https://elib.dlr.de/141315/.

[50] M. Holst, S. Aschbrenner, et al., Cost forecast for low-temperature electrolysis – technology driven bottom-up prognosis for PEM and alkaline water electrolysis systems, Fraunhofer Institute for Solar Energy Systems ISE (2021), https://doi.org/10.24406/publica-1318.
[51] M. Stanitsas, K. Kirytopoulos, Sustainable Energy strategies for power purchase agreements (PPAs), Sustainability 15 (2023) 6638, https://doi.org/10.3390/su15086638.
[52] enervis energy advisors GmbH. *enervis PPA-Preistracker*. [Last accessed on Dec. 18, 2024]. Available from: https://enervis.de/leistung/ppa-preistracker/.
[53] Amprion GmbH. *Grid Charges*. [Last accessed on Dec. 18, 2024]. Available from: https://www.amprion.net/Market/Grid-Customer/Grid-Charges/.
[54] Amprion GmbH. *Former grid charges*. [Last accessed on Dec. 18, 2024]. Available from: https://www.amprion.net/Market/Grid-Customer/Grid-Charges/Bisherige-Nutzungsentgelte-(informell).html.
[55] Landesamt für Natur, U.u.V.N.L. *Energieatlas NRW*. [Last accessed on Dec. 18, 2024]. Available from: https://www.energieatlas.nrw.de/site/bestandskarte.
[56] Pfenninger, S. and I. Staffell. *Renewables.ninja*. [Last accessed on Dec. 18, 2024]. Available from: https://www.renewables.ninja/.
[57] S. Pfenninger, I. Staffell, Long-term patterns of European PV output using 30 years of validated hourly reanalysis and satellite data, Energy 114 (2016) 1251–1265, https://doi.org/10.1016/j.energy.2016.08.060.
[58] I. Staffell, S. Pfenninger, Using bias-corrected reanalysis to simulate current and future wind power output, Energy 114 (2016) 1224–1239, https://doi.org/10.1016/j.energy.2016.08.068.
[59] Bundesnetzagentur für Elektrizität, G., Telekommunikation, Post und Eisenbahnen, and Bundeskartellamt, *Monitoring report 2023*. 2023. Available from: https://data.bundesnetzagentur.de/Bundesnetzagentur/SharedDocs/Downloads/EN/Areas/ElectricityGas/CollectionCompanySpecificData/Monitoring/MonitoringReport2023.pdf.
[60] Erbach, G. and S. Svensson, EU rules for renewable hydrogen - delegated regulations on a methodology for renewable fuels of non-biological origin. 2023, European Parliamentary Research Service (EPRS). Available from: https://www.europarl.europa.eu/RegData/etudes/BRIE/2023/747085/EPRS_BRI(2023)747085_EN.pdf.
[61] International Renewable Energy Agency (IRENA), *Making the breakthrough: Green hydrogen policies and technology costs*. 2021: Abu Dhabi. Available from: https://www.irena.org/-/media/Files/IRENA/Agency/Publication/2020/Nov/IRENA_Green_Hydrogen_breakthrough_2021.pdf?la=en&hash=40FA5B8AD7AB1666EECBDE30EF458C45EE5A0AA6.
[62] M. Nasser, T.F. Megahed, et al., A review of water electrolysis–based systems for hydrogen production using hybrid/solar/wind energy systems, Environ. Sci. Pollut. Res. 29 (58) (2022) 86994–87018, https://doi.org/10.1007/s11356-022-23323-y.
[63] M. Robinius, P. Markewitz, et al., Kosteneffiziente und klimagerechte Transformationsstrategien für das deutsche Energiesystem bis zum Jahr 2050, Energie & Umwelt. 499 (2020). Forschungszentrum Jülich GmbH, Institut für Energie- und Klimaforschung Techno-ökonomische Systemanalyse (IEK-3). Available from: https://www.researchgate.net/publication/343601046_WEGE_FUR_DIE_ENERGIEWENDE_Kosteneffiziente_und_klimagerechte_Transformationsstrategien_fur_das_deutsche_Energiesystem_bis_zum_Jahr_2050.
[64] G. Brändle, M. Schönfisch, S. Schulte, Estimating long-term global supply costs for low-carbon hydrogen, Appl. Energy 302 (2021) 117481, https://doi.org/10.1016/j.apenergy.2021.117481.
[65] V. Jülch, Comparison of electricity storage options using levelized cost of storage (LCOS) method, Appl. Energy 183 (2016) 1594–1606, https://doi.org/10.1016/j.apenergy.2016.08.165.
[66] A. Smallbone, V. Jülch, et al., Levelised cost of storage for pumped heat Energy storage in comparison with other energy storage technologies, Energy Convers. Manag. 152 (2017) 221–228, https://doi.org/10.1016/j.enconman.2017.09.047.
[67] The MathWorks Inc. MATLAB Version*:* 9.9.0.1467703 *(R2020b)*. [Last accessed on Dec. 18, 2024]. Available from: https://www.mathworks.com.
[68] The MathWorks Inc. *fminsearch*. [Last accessed on Dec. 18, 2024]. Available from: https://www.mathworks.com/help/matlab/ref/fminsearch.html.
[69] The Society for the Advancement of Applied Computer Science. *TOP-Energy Version 3.1.0*. [Last accessed on Dec. 18, 2024]. Available from: https://www.top-energy.de/en.
[70] Gurobi. *Gurobi Optimizer*. [Last accessed on Dec. 18, 2024]. Available from: https://www.gurobi.com/products/gurobi-optimizer/.